Wavelet solvers for *hp*-FEM discretizations in 3D using hexahedral elements

Sven Beuchler*
Institute of Computational Mathematics
Johannes-Kepler University Linz
Altenberger Straße 69
A-4040 Linz, Austria
sven.beuchler@jku.at

October 18, 2007

Abstract

In this paper we investigate the discretization of an elliptic boundary value problem in 3D by means of the *hp*-version of the finite element method using a mesh of hexahedrons. The corresponding linear system is solved by a preconditioned conjugate gradient method with an overlapping preconditioner as inexact additive Schwarz preconditioner. The remaining subproblems are treated by a tensor product based preconditioner. This preconditioner uses a basis transformation into a basis which is stable in L_2 and H^1. Several numerical examples show the efficiency of the proposed method.

1 Introduction

In this paper, we investigate the following boundary value problem: Let $\Omega \subset \mathbb{R}^3$ be a bounded domain and let $f \in L_2(\Omega)$, $f_1 \in L_2(\partial\Omega)$. Find $u \in H^1_{\Gamma_1}(\Omega) = \{u \in H^1(\Omega), u = 0 \text{ on } \Gamma_1\}$, $\Gamma_1 \cap \Gamma_2 = \emptyset$, $\Gamma_1 \cup \Gamma_2 = \partial\Omega$ such that

$$a(u,v) := \int_\Omega (\nabla u)^\top \nabla v = \int_\Omega fv + \int_{\Gamma_2} f_1 v := \langle f, v\rangle_\Omega + \langle f_1, v\rangle_{\Gamma_2} \tag{1.1}$$

holds for all $v \in H^1_{\Gamma_1}(\Omega)$. Problem (1.1) will be discretized by means of the *hp*-version of the finite element method using hexahedral elements $\triangle_s$, $s = 1, \ldots, nel$. Let $\hat{\triangle} = (-1,1)^3$ be the reference hexahedron and $F_s : \hat{\triangle} \to \triangle_s$ be the isoparametric mapping to the element $\triangle_s$.
We define the finite element space $\mathbb{M} := \{u \in H^1_{\Gamma_1}(\Omega), u\,|_{\triangle_s} = \tilde{u}(F_s^{-1}(x,y,z)), \tilde{u} \in \mathbb{Q}_p\}$, where $\mathbb{Q}_p$ is the space of all polynomials of maximal degree p in each variable. By $[\mathtt{Z}] = (\zeta_1, \ldots, \zeta_N)$, we denote a basis for $\mathbb{M}$ in which the functions $\zeta_1, \ldots, \zeta_{n_v}$ are the usual hat functions. The functions $\zeta_{n_v+(j-1)(p-1)+1}, \ldots, \zeta_{n_v+j(p-1)}$ correspond to the edge e_j of the mesh, and vanish on all other edges, i.e. satisfy the condition $\zeta_{n_v+(j-1)(p-1)+k-1}\,|_{e_l} = \delta_{j,l} p_k$, where p_k is a polynomial of degree k, $k = 2, \ldots, p$. The support of an edge function is formed by those elements which have the corresponding edge e_j in common. One defines $\frac{(p-1)(p-2)}{2}$ face shapes which are polynomial on the

*This work has been supported by the Spezialforschungsbereich F013 "Numerical and Symbolic Scientific Computing" of the FWF, project F1306.

defining face and vanish on all other faces. The support of these face-based functions is formed by the two elements sharing the defining face. The remaining basis functions are interior bubble functions consisting of a support containing one element only. These functions vanish on each face of the mesh. With this definition, the basis functions ζ_i can be divided into four groups,

- the vertex functions (V),
- the edge bubble functions (E),
- face bubble functions (F),
- the interior bubble functions (I),

locally on each element $\triangle_s$, and globally on Ω.
The Galerkin projection of (1.1) onto $\mathbb{M}$ leads to the linear system of algebraic finite element equations

$$\mathcal{K}_\zeta \underline{u} = \underline{f}, \quad \text{where} \quad \mathcal{K}_\zeta = [a_\Delta(\zeta_j, \zeta_i)]_{i,j=1}^N, \quad \underline{f}_p = [\langle f, \zeta_i \rangle + \langle f_1, \zeta_i \rangle_{\Gamma_2}]_{i=1}^N . \tag{1.2}$$

Using the vector $\underline{u}$, an approximation $u_p = [\mathtt{Z}]\underline{u}$ of the exact solution u of (1.1) can be built from the usual finite element isomorphism. In the case of smooth solutions u in parts of the domain Ω, spectral methods, [17], and finite elements of high order (p-version), see e.g. [27], [28], [12] and the references therein, have become more and more popular for twenty years. For the h-version of the FEM, the polynomial degree p of the shape functions on the elements is kept constant and the mesh-size h is decreased. This is in contrast to the p-version of the FEM in which the polynomial degree p is increased and the mesh-size h is kept constant. Both ideas, mesh refinement and increasing the polynomial degree, can be combined. This is called the hp-version of the FEM. The advantage of the p-version in comparison to the h-version is that the solution converges faster to the exact solution with respect to the number of unknowns N. However, the solution of the system (1.2) is more difficult. The matrix $\mathcal{K}_\zeta$ and therefore the numerical solution of (1.2) depends on the choice of the basis functions and an appropriate preconditioner.
For $2 \leq i \leq p$, let

$$\hat{L}_i(x) = \frac{1}{2}\sqrt{(2i-3)(2i-1)(2i+1)} \int_{-1}^{x} L_{i-1}(s)\, \mathrm{d}s \tag{1.3}$$

be the i-th integrated Legendre polynomial where $L_i(x) = \frac{1}{2^i i!}\frac{\mathrm{d}^i}{\mathrm{d}x^i}(x^2-1)^i$ denotes the i-th Legendre polynomial. Moreover, let $\hat{L}_{0/1}(x) = \frac{1 \pm x}{2}$. In the case of parallelepipedal elements, the stiffness matrix with respect to the tensor products of the integrated Legendre polynomials (1.3) has $\mathcal{O}(p^3)$ nonzero matrix entries. Therefore, the solution time of the system (1.2) should require $\mathcal{O}(p^3)$ flops up to some logarithmic terms.
It is known from literature, see [29], that domain decomposition (DD) methods are a powerful tool for the development of parallel preconditioners for the h-version as well as for the p-version of the FEM. In the two-dimensional case, nonoverlapping DD preconditioners with inexact subproblem solvers on the subdomains are preferred since the coupling between the high order functions, i.e. edge bubbles and interior bubbles, and the vertex functions can be removed by paying a $\log p$ term in the condition number estimates, [2]. This preconditioner requires a solver related to the Dirichlet problem on the elements $\triangle_s$, see [19, 3, 6, 13], a solver related to the Schur complement corresponding to the subdomain boundaries, see [16, 1], and an approximate discrete harmonic extension from $\partial\triangle_s$ to $\triangle_s$, see [2, 22, 4, 8].
In the three-dimensional case, the situation is much more difficult due to the coupling between the face bubble (F), edge bubble (E) and vertex based functions (V). More precisely, a splitting into different spaces is not stable in the standard spaces, see e.g. [29]. Mandel, [20], suggested a

change of the subspaces. In [14], the space of the edge bubbles E has been changed to a modified space $\tilde{E}$. Based on the theoretical estimates in [24], [25], the stability proof has been obtained for the decomposition of the Schur complement related to the element boundaries into the Schur complement related to the face bubbles on each face separately and the wire-basket corresponding to vertex and edge bubble functions. In [6], see also [5] for the refined estimates, a first solver for the interior bubbles is developed in the basis of the integrated Legendre polynomials (1.3).
This solver uses a basis $[\Psi] = [\psi_{I,i}]_{i=2}^{p} \subset \mathbb{B}_{p,0} = \{u \in \mathbb{P}_p(-1,1), u(\pm 1) = 0\}$ which satisfies the following properties:

- There exist a diagonal matrix $\mathcal{D}_M$ and a diagonal matrix $\mathcal{D}_K$ such that the norm equivalences

$$\underline{u}^\top \mathcal{D}_K \underline{u} \sim \| [\Psi]\underline{u} \|^2_{H^1_0(-1,1)} \quad \text{and} \quad \underline{u}^\top \mathcal{D}_M \underline{u} \sim \| [\Psi]\underline{u} \|^2_{L_2(-1,1)} \tag{1.4}$$

  hold for all $\underline{u} \in \mathbb{R}^{p-1}$, where the constants do not depend on p.

- The basis transformation from the basis of the integrated Legendre polynomials into the basis $[\Psi]$ requires $\mathcal{O}(p)$ operations.

The basis $[\Psi]$ is called p-wavelet basis. In [18], a first preconditioner is proposed on the face bubbles based on multi-resolution analysis, see [6]. The wire basket is solved optimally with respect to the polynomial degree but not with respect to the number of elements. Based on the optimal solvers for the interior bubbles and the face bubbles, the approximate discrete harmonic extensions are replaced by nearly exact solutions for the interior bubbles. This is optimal due to the arithmetical complexity, a direct application of an explicit extension operator is much faster. Another approach is using overlapping preconditioners as developed in [23], see also [21] for the tetrahedral case. This avoids the usage of difficult extension operators. Moreover, the part of the system which corresponds to the h-part is decoupled from the p-part of the system. The overlapping preconditioner, which was proposed by Pavarino [23], requires only the solution of high-order systems on patches consisting of about 8 hexahedrons. It is necessary to use polynomial degrees p between 10 and 20 on some elements, see [12] for some examples. Therefore, we need a solver for a patch structure with relatively high polynomial degree.
In this paper, we propose fast solvers for the patch structure. The total complexity for the solution of the system of linear algebraic equations is $\mathcal{O}(p^3 \log^\kappa p)$ with $\kappa < 2$, i.e. quasioptimal with respect to the number of unknowns. The main goal is the development of another p-wavelet basis with properties as in (1.4) for spaces of the type $\mathbb{B}_{p,1} = \{u \in \mathbb{P}_p(-1,1), u(1) = 0\}$. This is an extension of the results presented in [6], [5]. Moreover, the solvers use the tensor product structure of the elements and patches directly.
The outline of this paper is as follows. Section 2 explains the Pavarino preconditioner. Moreover, we determine the corresponding one-dimensional model problem of the tensor product structure. The main part of this paper is Section 3. Here, we investigate several wavelet preconditioners for this one-dimensional model problem based on norm equivalences as in (1.4). In Section 4, we define the solver related to the patches. Furthermore, several numerical experiments show the efficiency of the proposed method. This includes also the comparison to direct solvers. Section 5 is devoted to possible generalizations of the presented results and concludes the work.
Throughout this paper, the integer p denotes the polynomial degree. For two real symmetric and positive definite $n \times n$ matrices A, B, the relation $A \preceq B$ means that $A - cB$ is negative definite, where $c > 0$ is a constant independent of n, or p. The relation $A \sim B$ means $A \preceq B$ and $B \preceq A$, i.e. the matrices A and B are spectrally equivalent. The isomorphism between a function $u = \sum_i u_i \psi_i \in L^2$ and the vector of coefficients $\underline{u} = [u_i]_i$ with respect to the basis $[\Psi] = [\psi_1, \psi_2, \ldots]$ is denoted as $u = [\Psi]\underline{u}$.

2 Domain decomposition

In this section, we present an overlapping preconditioner which has been developed by Pavarino, [23]. It decouples the h-part of the system from the p-part system. For the definition of the preconditioner, some notation is introduced. Let

$$\mathbb{V}_0 = \left\{ u \in H^1_{\Gamma_1}(\Omega), u \mid_{\triangle_s} = \tilde{u}(F_s^{-1}(x,y,z)), \tilde{u} \in \mathbb{Q}_1 \right\} \tag{2.1}$$

be the space of all finite element functions of maximal polynomial degree 1. Moreover, let

$$\Omega_v = \{ \cup_s \overline{\triangle}_s, v \subset \overline{\triangle}_s \}$$

be the closed patch to a node v of the finite element mesh. Then, for each node v of the finite element mesh, we introduce

$$\mathbb{V}_v = \{ u \in \mathbb{M}, \text{supp } u \subset \Omega_v \} \tag{2.2}$$

as the patch space, cf. Figure 1.

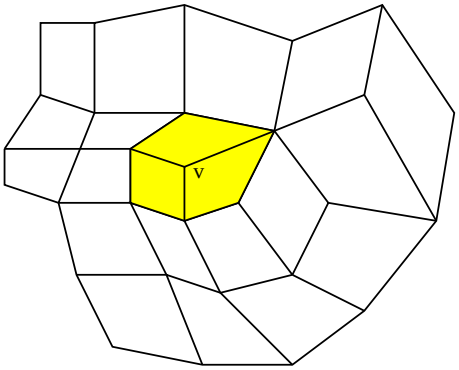

Figure 1: Patch Ω_v of a node v (2D).

Theorem 2.1. *Let $\mathbb{V}_v$ and $\mathbb{V}_0$ be defined via (2.2) and (2.1), respectively. Then, we have*

$$a(u,u) \sim a(u_0,u_0) + \sum_v a(u_v,u_v), \quad \forall u = u_0 + \sum_v u_v, u_0 \in \mathbb{V}_0, u_v \in \mathbb{V}_v.$$

The constants depend neither on h nor on p.

Proof. This result has been proved by Pavarino [23]. □

Therefore, it suffices to solve systems on the subspaces $\mathbb{V}_0$ and $\mathbb{V}_v$ where v is running over all nodes v. The system on $\mathbb{V}_0$ corresponds to the h-part of the global system. Here, many solvers in the sense of inexact additive Schwarz preconditioners are available in order to solve the system in optimal arithmetical complexity. Examples are multigrid methods, [15], and the BPX-preconditioner, [7], for structured meshes and algebraic multigrid methods (AMG) for unstructured meshes.
For low local polynomial degrees, the systems related to $\mathbb{V}_v$ can be handled by a direct solver. However, if the local polynomial degree p is increasing, this is too expensive, cf. Table 1 for the dimensions of the local subspaces. Therefore, if p is large, an iterative solver with a suitable preconditioner should be preferred. In the standard case, a patch consists of eight hexahedrons ($2 \times 2 \times 2$). Moreover, a moderate deformation of the hexahedrons into unit cubes leads to a spectrally equivalent system with respect to the polynomial degree. The condition number depends

p	1	3	5	7	9	11	13
Dimension of $\mathbb{V}_v$	1	125	729	2197	4913	9261	15625

Table 1: Dimension of $\mathbb{V}_v$ for a patch of $2 \times 2 \times 2$ cubes.

only on the angles of the involved, possibly curvilinear, elements $\triangle_s$, [16]. Hence, the situation with $2 \times 2 \times 2$ cubes and Dirichlet boundary conditions is the typical model problem in order to derive a solver for $\mathbb{V}_v$ for high p.
This problem has a tensor product structure. The corresponding one-dimensional problem is the situation with two elements, i.e. the intervals $(-2, 0)$ and $(0, 2)$ and Dirichlet boundary conditions at $x = \pm 2$, i.e. find $u \in \mathbb{B}_p = \{u \in H_0^1(-2, 2), u\,|_{(-2,0)} \in \mathbb{P}_p, u\,|_{(0,2)} \in \mathbb{P}_p\}$ such that

$$\int_{-2}^{2} u'v' \,\mathrm{d}x + \int_{-2}^{2} uv \,\mathrm{d}x = g \quad \forall v \in \mathbb{B}_p. \tag{2.3}$$

Let $[\Phi_p]$ be some basis of $\mathbb{B}_p$. Then, the solution of (2.3) is equivalent to the solution of the linear system $(K^{\Phi_p} + M^{\Phi_p})\underline{u} = \underline{g}$ with the mass and stiffness matrix

$$K^{\Phi_p} = \int_{-2}^{2} \frac{\mathrm{d}}{\mathrm{d}x}[\Phi_p]^\top \frac{\mathrm{d}}{\mathrm{d}x}[\Phi_p] \,\mathrm{d}x \quad \text{and} \quad M^{\Phi_p} = \int_{-2}^{2} [\Phi_p]^\top [\Phi_p] \,\mathrm{d}x, \tag{2.4}$$

respectively. Then the solution of the model problem for $\mathbb{V}_v$ is the solution of a system with the matrix

$$K_3 = K^{\Phi_p} \otimes M^{\Phi_p} \otimes M^{\Phi_p} + M^{\Phi_p} \otimes K^{\Phi_p} \otimes M^{\Phi_p} + M^{\Phi_p} \otimes M^{\Phi_p} \otimes K^{\Phi_p}. \tag{2.5}$$

Our aim is to derive preconditioners $\mathfrak{C}_M$ and $\mathfrak{C}_K$ for M^{Φ_p} and K^{Φ_p}, respectively. These preconditioners are of the form

$$\mathfrak{C}_M^{-1} = W \mathfrak{D}_M^{-1} W^\top \quad \text{and} \quad \mathfrak{C}_K^{-1} = W \mathfrak{D}_K^{-1} W^\top, \tag{2.6}$$

where the multiplications $W\underline{u}$ and $W^\top \underline{u}$ require $\mathcal{O}(p)$ floating point operations, and the matrices $\mathfrak{D}_M$ and $\mathfrak{D}_K$ are diagonal matrices. Then, the matrix C_3, which is defined via

$$C_3^{-1} = (W \otimes W \otimes W)(\mathfrak{D}_K \otimes \mathfrak{D}_M \otimes \mathfrak{D}_M + \mathfrak{D}_M \otimes \mathfrak{D}_K \otimes \mathfrak{D}_M + \mathfrak{D}_M \otimes \mathfrak{D}_M \otimes \mathfrak{D}_K)^{-1} (W \otimes W \otimes W)^\top, \tag{2.7}$$

is a preconditioner for K_3 (2.5), where the action $C_3^{-1}\underline{r}$ requires $\mathcal{O}(p^3)$ floating point operations. In the next section, we derive the preconditioners (2.6). In Section 4, we return to the three-dimensional problem.

3 The one-dimensional model problem

In this section, we consider problem (2.3). In subsection 3.1, we define a basis of the space $\mathbb{B}_p$. Moreover, we give some interpretations of the mass and stiffness matrix (2.4) as discretization matrices for the h-version of the FEM. Subsections 3.2 and 3.3 consider wavelet solvers on the one-dimensional reference element $(-1, 1)$ and for problem (2.3), respectively.

3.1 Structure of mass and stiffness matrix

3.1.1 Definition of the basis functions

In order to determine mass and stiffness matrix, we have to specify our basis functions of the space $\mathbb{B}_p$. First, the functions on the reference interval $(-1, 1)$ are defined. For reasons of simplicity, let

us assume that p is odd. Now, we define

$$\tilde{L}_i(x) := \sqrt{\frac{(2i-1)}{4(2i-3)(2i+1)}}\hat{L}_i(x) = \frac{1}{4}(2i-1)\int_{-1}^{x} L_{i-1}(s)\,\mathrm{d}s, \quad i \geq 2 \tag{3.1}$$

as the i-th integrated Legendre polynomial in $[-1,1]$ with another scaling as in (1.3). Moreover, let $\tilde{L}_{0/1}(x) := \frac{1\pm x}{2}$.
The local functions on the elements $(0,2)$ and $(-2,0)$ are obtained by the affine translation $y = x \pm 1$. This defines the basis functions on $\mathbb{B}_p$, i.e.

$$\begin{aligned}
\tilde{\phi}_1(x) &= \frac{1}{2}\begin{cases} 2+x & x \in [-2,0] \\ 2-x & x \in [0,2] \\ 0 & \text{else} \end{cases}, \\
\tilde{\phi}_i(x+1) &= \begin{cases} \tilde{L}_i(x) & |x| \leq 1 \\ 0 & \text{else} \end{cases}, i = 2,\ldots,p, \\
\tilde{\phi}_{p+i-1}(x-1) &= \begin{cases} (-1)^i\tilde{L}_i(x) & |x| \leq 1 \\ 0 & \text{else} \end{cases}, i = 2,\ldots,p
\end{aligned} \tag{3.2}$$

where $[\tilde{L}]$ denotes the integrated Legendre polynomials (3.1). Then

$$[\tilde{L}_{(-2,2)}] = \left[\tilde{\phi}_i\right]_{i=1}^{2p-1} \tag{3.3}$$

forms a basis of $\mathbb{B}_p$. The matrices

$$K^{\tilde{L}_{(-2,2)}} = \int_{-2}^{2} \frac{\mathrm{d}}{\mathrm{d}x}[\tilde{L}_{(-2,2)}]^\top \frac{\mathrm{d}}{\mathrm{d}x}[\tilde{L}_{(-2,2)}]\,\mathrm{d}x \quad \text{and} \quad M^{\tilde{L}_{(-2,2)}} = \int_{-2}^{2} [\tilde{L}_{(-2,2)}]^\top [\tilde{L}_{(-2,2)}]\,\mathrm{d}x \tag{3.4}$$

are the result of assembling the local stiffness and mass matrices on the two intervals $(-2,0)$ and $(0,2)$. In order to compute the entries of the matrices in (3.4), we have to consider the matrices on the reference element $(-1,1)$. Note that the structure of the space $\mathbb{B}_p$ with the Dirichlet boundary conditions at $x = \pm 2$ implies that exactly one hat function is required on each of the two elements. Using the properties of the integrated Legendre polynomials, the mass and stiffness matrix on the reference interval $(-1,1)$ can be computed explicitly. In order to get some structure in the matrices, the integrated Legendre polynomials (3.1) are ordered in the following way:

- first the odd polynomials starting from the highest polynomial,
- then one of the hat functions, i.e. $\tilde{L}_1(x)$ or $\tilde{L}_0(x)$,
- and finally the even polynomials starting from the lowest polynomial,

e.g.

$$[\tilde{L}_{(-1,1)}] = \left[\tilde{L}_p, \tilde{L}_{p-2}, \ldots, \tilde{L}_3(x), \tilde{L}_1(x), \tilde{L}_2(x), \tilde{L}_4(x), \ldots \tilde{L}_{p-1}(x)\right] \tag{3.5}$$

Consequently for the Dirichlet boundary condition on $(-1,1)$ at $x=-1$, we have

$$M^{\tilde{L}_{(-1,1)}} := \int_{-1}^{1} [\tilde{L}_{(-1,1)}]^\top [\tilde{L}_{(-1,1)}] \,\mathrm{d}x \tag{3.6}$$

$$= \frac{1}{4}\begin{bmatrix}
\frac{2}{2p+1}+\frac{2}{2p-3} & -\frac{2}{2p-3} & 0 & \dots & & & & \dots & 0 \\
 & \ddots & & \ddots & & & & & \vdots \\
0 & -\frac{2}{11} & \frac{2}{7}+\frac{2}{11} & -\frac{2}{7} & 0 & 0 & 0 & \dots & 0 \\
\dots & 0 & -\frac{2}{7} & \frac{2}{7}+\frac{2}{3} & -\frac{2}{3} & 0 & 0 & \dots & 0 \\
0 & \dots & 0 & -\frac{2}{3} & \frac{8}{3} & -2 & 0 & \dots & 0 \\
0 & & \dots & 0 & -2 & \frac{12}{5} & -\frac{2}{5} & 0 & \dots \\
0 & & & \dots & 0 & -\frac{2}{5} & \frac{2}{9}+\frac{2}{5} & -\frac{2}{9} & 0 \\
\vdots & & & & & \ddots & & \ddots & \vdots \\
0 & \dots & & & & \dots & 0 & -\frac{2}{2p-5} & \frac{2}{2p-5}+\frac{2}{2p-1}
\end{bmatrix}.$$

Moreover, the orthogonality of the Legendre polynomials implies

$$\begin{aligned} K^{\tilde{L}_{(-1,1)}} &:= \int_{-1}^{1} \frac{\mathrm{d}}{\mathrm{d}x}[\tilde{L}_{(-1,1)}]^\top \frac{\mathrm{d}}{\mathrm{d}x}[\tilde{L}_{(-1,1)}] \,\mathrm{d}x \\ &= \frac{1}{4}\mathrm{diag}\,[4p-2, 4p-10, \dots, 18, 10, 2, 6, 14, \dots, 4p-14, 4p-6]\,. \end{aligned} \tag{3.7}$$

In the case the Dirichlet boundary condition on $(-1,1)$ at $x=1$, we replace $[\tilde{L}_{(-1,1)}]$ by the modified basis $[\Phi_{0,p}] = \left[-\tilde{L}_p(x), -\tilde{L}_{p-2}(x), \dots, -\tilde{L}_3(x), \tilde{L}_0(x), \tilde{L}_2(x), \tilde{L}_4(x), \dots \tilde{L}_{p-1}(x)\right]$ see (3.2) and obtain the same result for mass and stiffness matrix as in (3.6), (3.7). The matrices $M^{\tilde{L}_{(-2,2)}}$ and $K^{\tilde{L}_{(-2,2)}}$ (3.4) are obtained by a simple assembling of $M^{\tilde{L}_{(-1,1)}}$ (3.6) and $K^{\tilde{L}_{(-1,1)}}$ (3.7). For $p=7$, the matrices and all shape functions of $\mathbb{B}_p$ are displayed in Appendix A.

3.1.2 Interpretations of mass and stiffness matrix

The solvers presented in [6] based on the norm equivalences (1.4) use h-FEM interpretations of the corresponding mass and stiffness matrix in the basis of the integrated Legendre polynomials. A similar approach is possible for K_1 (3.7) and M_1 (3.6), respectively. However, we have to modify the corresponding weight functions. The matrix M_1 is a weakly diagonal dominant, tridiagonal and positive definite matrix with negative off diagonal entries. Hence, this matrix is also a stiffness matrix for an h-FEM method on the unit interval with an appropriate weight function specified below. Moreover, we derive a spectrally equivalent matrix for K_1 (3.7) that is a mass matrix for an h-FEM method and an appropriate weight function ω on the unit interval $[-1,1]$. For this reason, we even abandon the diagonal structure and admit diagonally dominant tridiagonal matrices.
To this end, we study the following auxiliary variational problem:
Let

$$\begin{aligned} H^1_{\omega_1,\omega_2}(-1,1) &:= \{u \in L^2(-1,1), u(\pm 1) = 0, \int_{-1}^{1} \omega_2^2(x) u^2(x) \,\mathrm{d}x < \infty, \\ &\qquad \int_{-1}^{1} \omega_1^2(x)(u')^2(x) \,\mathrm{d}x < \infty\}. \end{aligned}$$

Find $u \in H^1_{\omega_1,\omega_2}(-1,1)$ such that

$$a_1(u,v) = \langle u, v\rangle_{\omega_2} + \langle u', v'\rangle_{\omega_1} = \langle g, v\rangle \tag{3.8}$$

holds for all $v \in H^1_{\omega_1,\omega_2}(-1,1)$, where

$$\langle u, v\rangle_\omega := \int_{-1}^{1} \omega^2(x)u(x)v(x)\,\mathrm{d}x \quad \text{and} \quad \| v \|^2_\omega := \langle v, v\rangle_\omega. \tag{3.9}$$

The weight functions ω_i, $i = 1, 2$ will be specified later. The one-dimensional problem (3.8) is discretized by linear finite elements on the equidistant mesh $T_n = \bigcup_{i=-n}^{n-1} \tau_i^n$ where $\tau_i^n = \left(\frac{i}{n}, \frac{i+1}{n}\right)$ and $n = \frac{p+1}{2}$. The one-dimensional hat functions on this mesh,

$$\phi_i^n(x) = \begin{cases} nx - (i-1) & \text{on } \tau_{i-1}^n, \\ (i+1) - nx & \text{on } \tau_i^n, \\ 0 & \text{otherwise,} \end{cases} \qquad i = -n+1, \ldots, n-1, \tag{3.10}$$

are a basis of the finite element space $\mathbb{V}_n = \mathrm{span}[\phi_i^n]_{i=-n+1}^{n-1} = \mathrm{span}[\Phi_n^1]$. The Galerkin projection onto $\mathbb{V}_n$ for (3.8) can be described as follows: Find $u^n \in \mathbb{V}_n$ such that

$$a_1(u^n, v^n) = \langle g, v^n\rangle \quad \forall v^n \in \mathbb{V}_n. \tag{3.11}$$

This gives rise to the linear equation $(K^\phi_{\omega_1} + M^\phi_{\omega_2})\underline{u} = \underline{g}$ with

$$K^\phi_{\omega_1} := \left[\langle (\phi_j^n)', (\phi_i^n)'\rangle_{\omega_1}\right]_{i,j=-n+1}^{n-1} \quad \text{and} \quad M^\phi_{\omega_2} := \left[\langle \phi_j^n, \phi_i^n\rangle_{\omega_2}\right]_{i,j=-n+1}^{n-1}. \tag{3.12}$$

Then, $u^n = \sum_{i=-n+1}^{n-1} \phi_i^n \underline{u}_i := [\Phi_n^1]\underline{u}$ is the solution of (3.11).
We prove now the following result.

Lemma 3.1. *Let $n = \frac{p+1}{2}$. Let $K^{\tilde{L}_{(-1,1)}}$ be defined according to* (3.7)*. Then we have the spectral equivalence*

$$K^{\tilde{L}_{(-1,1)}} \sim n^2 M^\phi_{\omega_2(x)=\sqrt{|x|}}. \tag{3.13}$$

Proof. We compute the element stiffness matrix $M^\phi_{\omega_2,i}$ on the element τ_i, $i \geq 1$ and obtain

$$M^\phi_{\omega_2,i} = \frac{1}{12n^2}\begin{bmatrix} 4i-3 & 2i-1 \\ 2i-1 & 4i+1 \end{bmatrix}.$$

We define

$$\tilde{F}_i = \frac{1}{12n^2}\begin{bmatrix} 4i-3 & 0 \\ 0 & 4i+1 \end{bmatrix} \quad \text{and} \quad F_i = \frac{1}{12n^2}\begin{bmatrix} 4i-3 & 0 \\ 0 & 4i-1 \end{bmatrix}.$$

Since $\frac{2i-1}{\sqrt{(4i-3)(4i+1)}} \geq \frac{2i-1}{4i-1} \geq \frac{1}{2}$ for $i \geq 1$, we can conclude that

$$\frac{1}{2}\tilde{F}_i \leq M^\phi_{\omega_2.i} \leq \frac{3}{2}\tilde{F}_i, \quad i \geq 1. \tag{3.14}$$

Moreover, a simple computation shows that

$$\frac{3}{5}\tilde{F}_i \leq F_i \leq \tilde{F}_i, \quad i \geq 1. \tag{3.15}$$

Combining (3.14) and (3.15), we have $\frac{1}{2}F_i \leq M^\phi_{\omega_2,i} \leq \frac{5}{2}F_i$. By symmetry of the weight function, we have $M^\phi_{\omega_2,i} = M^\phi_{\omega_2,-i+1}$. The assembling of $M^\phi_{\omega_2,i}$ yields to $M^\phi_{\omega_2}$, whereas the assembling of F_i gives the matrix

$$F = \mathrm{diag}\,[4p+4, 4p-4, \ldots, 16, 8, 2, 8, 16, \ldots, 4p-4, 4p+4] \in \mathbb{R}^{2n-1,2n-1}.$$

Since $F \sim K^{\tilde{L}_{(-1,1)}}$, the assertion follows by an argument for assembled matrices, [30]. □

For the matrix $M^{\tilde{L}_{(-1,1)}}$ (3.6), a similar result can be shown. However, we have to introduce the discrete weight function ω_1

$$\omega_1(x) = \begin{cases} \frac{1}{\sqrt{|x|}} & \text{if} \quad |x| > \frac{1}{n} \\ \sqrt{|n|} & \text{if} \quad |x| \leq \frac{1}{n} \end{cases} . \tag{3.16}$$

Lemma 3.2. *Let ω_1 be defined by* (3.16)*. Moreover, let $K^{\phi}_{\omega_1}$ and $M^{\tilde{L}_{(-1,1)}}$ be defined by* (3.12) *and* (3.7)*, respectively. Then, we have $K^{\phi}_{\omega_1} \sim n^2 M^{\tilde{L}_{(-1,1)}}$.*

Proof. As in the proof of the previous Lemma 3.1, the assertion follows from the structure of the local stiffness matrices, [30]. □

Remark 3.3. *In [6], we have chosen differently scaled integrated Legendre polynomials $\hat{L}_i(x)$* (1.3)*. In that case, a similar interpretation of the mass and the stiffness matrix is possible. The disadvantage of the functions $\hat{L}_i(x)$ is that this approach is limited to the interior bubbles. If one of the hat functions $\frac{1\pm x}{2}$ is added to the basis functions, the p-FEM mass matrix looses its dominance on the diagonal. Hence, a similar interpretation which also includes one hat function is not possible in the basis of the $[\hat{L}_i]_i$.*

Remark 3.4. *For the parts of $M^{\tilde{L}_{(-1,1)}}$* (3.6) *and $K^{\tilde{L}_{(-1,1)}}$* (3.7) *which correspond to the even polynomials, similar interpretations are possible. It is only necessary to replace the interval $(-1,1)$ in* (3.9) *by $(0,1)$ and to introduce a Neumann boundary condition at $x = 0$. More precisely, the matrices*

$$M^{\tilde{L}_{(-1,1)}}_{even} := \frac{1}{4}\begin{bmatrix} 2 & -2 & 0 & \dots & 0 \\ -2 & 2+\frac{2}{5} & -\frac{2}{5} & 0 & \dots \\ 0 & -\frac{2}{5} & \frac{2}{9}+\frac{2}{5} & -\frac{2}{9} & 0 \\ \vdots & \ddots & & \ddots & \vdots \\ 0 & \dots & 0 & -\frac{2}{2p-5} & \frac{2}{2p-5}+\frac{2}{2p-1} \end{bmatrix} \quad \textit{and}$$

$$K^{\tilde{L}_{(-1,1)}}_{even} := \frac{1}{4}\mathrm{diag}\,[2, 6, 14, \dots, 4p-14, 4p-6]$$

are the matrices for the even part. The above interpretations follow now by the same arguments.

3.2 Wavelet solver on one element

In view of (2.5) and Lemmas 3.1 and 3.2, our goal is to derive preconditioners for Kronecker products between a weighted stiffness matrix, i.e. $K^{\phi}_{\omega_1}$ (3.16) (or $M^{\tilde{L}_{(-1,1)}}$), and a weighted mass matrix, i.e. $M_{\omega_2=\sqrt{|x|}}$ (3.12) (or $K^{\tilde{L}_{(-1,1)}}$). Our approach is using wavelet preconditioners. Similar to (2.6), we consider preconditioners C_M^{-1} and C_K^{-1} for $M^{\tilde{L}_{(-1,1)}}$ (3.6) and $K^{\tilde{L}_{(-1,1)}}$ (3.7), respectively, which are of the form

$$C_M^{-1} = Q_k D_M^{-1} Q_k^{\top} \quad \text{and} \quad C_K^{-1} = Q_k D_K^{-1} Q_k^{\top}.$$

The matrices D_M and D_K are proper diagonal or blockdiagonal matrices. The matrix Q_k corresponds to the wavelet basis transformation, i.e.

$$[\Psi_k] = [\psi_j^l]_{(j,l)\in\hat{I}_k} = [\Phi_n^1] Q_k,$$

where the index set $\hat{I}_k$ is defined by

$$\hat{I}_k = \left\{(i,l) \in \mathbb{N}^2,\ 1 \leq l \leq k,\ i = 2m-1,\ -2^{l-1} \leq m \leq 2^{l-1},\ m \in \mathbb{N}\right\}; \tag{3.17}$$

see [9, 26, 10]. The index k denotes the level number, i.e. $n = 2^k$.
In subsubsection 3.2.1, we present theoretical estimates which show that wavelet preconditioners for $K^{\tilde{L}_{(-1,1)}}$ and $M^{\tilde{L}_{(-1,1)}}$ lead to quasioptimal solvers. In subsubsection 3.2.2, we present some numerical results which confirm the theoretical estimates. In subsubsection 3.2.3, a modified wavelet solver is developed. This solver decreases the condition number of the preconditioned systems with out loss of arithmetical complexity.

3.2.1 Condition number estimates

For getting a wavelet preconditioner for the matrix $M^{\phi}_{\omega_2}$ (3.12) we have to deal with the mass matrix $M^{\phi}_{\omega(x)=\sqrt{|x|}}$ for a singular weight at $x = 0$. First, we consider the case of the interval $(0, 1)$ with Neumann boundary conditions at the singularity $x = 0$ and the weight $\omega_2(x) = \sqrt{x}$.
Let

$$\hat{I}_{k,+} = \left\{(i,l) \in \mathbb{N}^2,\ 1 \le l \le k,\ i = 2m-1,\ 0 \le m \le 2^{l-1},\ m \in \mathbb{N}\right\}.$$

For $\alpha \in \mathbb{R}$, let $\omega(x) = x^{\alpha}$ be a weight function and $M^{\psi,\infty}_{\omega_2}$ be the infinite matrix

$$M^{\psi,\infty}_{\omega} = \left[\int_0^1 \omega^2(x)\psi^l_j(x)\psi^{l'}_{j'}(x)\,\mathrm{d}x\right]_{(j,l),(j',l')\in\cup_{k=1}^{\infty}\hat{I}_{k,+}}. \tag{3.18}$$

In general this matrix is not diagonal when we have a wavelet basis.
Following [6] we require some properties of the wavelets.

Assumption 3.5. *Let $[\Psi] = \left[\psi^l_j\right]_{(j,l)\in\cup_{k=1}^{\infty}\hat{I}_{k,+}}$ be a basis of $L^2(0,1)$ with piecewise linear functions ψ^l_j. There is a biorthogonal, or dual, Riesz basis $[\tilde{\Psi}] = \left[\tilde{\psi}^l_j\right]_{(j,l)}$ such that*

- $\left(\tilde{\psi}^l_j, \psi^{l'}_{j'}\right) = \delta_{j,j'}\delta_{l,l'}$,
- $\psi^l_j \in \mathbb{W}^0 \subset W^{1,\infty}(0,1)$, *and* $\tilde{\psi}^l_j \in \tilde{\mathbb{W}}^0 \subset W^{1,\infty}(0,1)$.

Furthermore, every $v \in L^2(0,1)$ has a representation

$$v = \sum_{l=1}^{\infty}\sum_j \langle v, \psi^l_j\rangle\tilde{\psi}^l_j = \sum_{l=1}^{\infty}\sum_j \langle v, \tilde{\psi}^l_j\rangle\psi^l_j = \sum_{1}^{\infty}\sum_j v^l_j\psi^l_j = [\Psi]\underline{v},$$

and the following norm equivalences hold:

$$\begin{aligned}
\|v\|_0^2 &\sim \sum_{l=1}^{\infty}\sum_j |\langle v, \psi^l_j\rangle|^2 \sim \sum_{l=1}^{\infty}\sum_j |\langle v, \tilde{\psi}^l_j\rangle|^2,\\
|v|_1^2 &\sim \sum_{l=1}^{\infty} 2^{2l}\sum_j |\left(v, \tilde{\psi}^l_j\right)|^2 = \sum_{l=1}^{\infty} 2^{2l}\sum_j v^l_j\,.
\end{aligned} \tag{3.19}$$

We have proved the following result.

Theorem 3.6. *For $\alpha \in \mathbb{R}$, let $\omega(x) = x^{\alpha}$ be a weight function and let $[\Psi]$ be a wavelet basis which satisfies Assumption 3.5. Moreover, let $M^{\Psi,\infty}_{\omega}$ be defined via* (3.18)*. If*

- *all piecewise linear functions ψ^l_j with $0 \in \operatorname{supp}\ \psi^l_j$ satisfy $\psi^l_j(0) = 0$ and $\alpha > -\frac{3}{2}$, or*
- $\alpha > -\frac{1}{2}$,

then we have

$$M_{\omega}^{\Psi,\infty} \preceq \operatorname{diag}\left[\max\{\omega^2(2^{-l}j), \omega^2(2^{-l-1})\}\right].$$

Proof. The proof has been given in [6, Theorem 3.2]. □

Therefore, we introduce the preconditioner

$$C_M^{-1} = Q_k D_M^{-1} Q_k^{\top} \quad \text{with} \quad D_M = \operatorname{diag}\left[\max\{\omega_2^2(2^{-l}j), \omega_2^2(2^{-l-1})\}\right] \tag{3.20}$$

for $M_{\omega_2=\sqrt{x}}^{\phi}$ (3.12).

Theorem 3.7. *Let the assumptions of Theorem 3.6 be satisfied. Moreover, let $M_{\omega_2=\sqrt{x}}^{\phi}$ and C_M^{-1} be defined as in* (3.12) *and* (3.20)*, where the integral runs from $(0,1)$ instead of $(-1,1)$, respectively. Then for any $\chi > 1$, we have*

$$\frac{1}{\log n \log^{\chi} \log n} C_M \preceq M_{\omega_2=\sqrt{x}}^{\phi} \preceq C_M. \tag{3.21}$$

Proof. We give only a sketch of the proof. A detailed proof requires several technical lemmas as in [6] and will be presented in a forthcoming paper.
The upper estimate follows from Theorem 3.6 with $\alpha = \frac{1}{2}$. For the lower estimate, an application of this theorem is not possible. Instead of the weight $\omega_2^2(x) = x$, we consider the modified weight $\tilde{\omega}_2^2(x) = x \log|2x| \log^{\chi} \log|2x|$ with some $\chi > 1$ and introduce the mass matrix

$$M_{\tilde{\omega}_2}^{\phi} := \left[\langle \phi_j^n, \phi_i^n \rangle_{\tilde{\omega}_2,(0,1)}\right]_{i,j=0}^{n-1}.$$

The definition of the weight functions ω_2 and $\tilde{\omega}_2$ implies the estimate

$$M_{\omega_2}^{\phi} \succeq \frac{1}{\log n \log^{\chi} \log n} M_{\tilde{\omega}_2}^{\phi}.$$

The biorthogonality of the wavelets implies

$$M_{\tilde{\omega}_2}^{\Psi,\infty} = \left(M_{(\tilde{\omega}_2)^{-1}}^{\Psi,\infty}\right)^{-1}$$

For the matrix $M_{(\tilde{\omega}_2)^{-1}}^{\phi}$, we are able to apply the above Theorem 3.6 with the dual weight function $\widetilde{\omega}_2^{-1}(x) = \dfrac{1}{x \log|2x| \log^{\chi} \log|2x|}$. Finally, we obtain

$$Q_k^{-\top} D_{\tilde{M}} Q_k^{-1} \preceq M_{\tilde{\omega}_2}^{\phi} \quad \text{with} \quad D_{\tilde{M}} = \operatorname{diag}\left[\max\{\tilde{\omega}_2^2(2^{-l}j), \tilde{\omega}_2(2^{-l-1})\}\right].$$

Since $\omega_2(x) \preceq \tilde{\omega}_2(x)$, we have $D_M \preceq D_{\tilde{M}}$ which implies $C_M = Q_k^{-\top} D_M Q_k^{-1} \preceq Q_k^{-\top} D_{\tilde{M}} Q_K^{-1}$. This gives the lower estimate. □

Next, we consider the wavelet preconditioner for $K_{\omega_1}^{\phi}$ (3.16).

$$C_K^{-1} = Q_k D_K^{-1} Q_k^{\top} \quad \text{with} \quad D_K = \operatorname{diag}\left[2^{2l} \omega_1^2(2^{-l}j)\right] \tag{3.22}$$

be the preconditioner for $K_{\omega_1}^{\phi}$ (3.16).

Theorem 3.8. *Let us assume that the assumptions of Theorem 3.6 are satisfied. Moreover, let $K_{\omega_1}^{\phi}$ and C_K^{-1} be defined via* (3.16) *and* (3.22)*, respectively. Then for any $\chi > 1$, we have*

$$C_K \preceq K_{\omega_1}^{\phi} \preceq \log n \log^{\chi} \log n \, C_K. \tag{3.23}$$

Proof. As in the proof of Theorem 3.7, only the idea of the proof is presented. The lower estimate follows directly from Theorem 3.6 applied to the dual weight $\frac{1}{\omega_1(x)} = x$. For the upper estimate, we introduce the matrix

$$K^{\phi}_{\tilde{\omega}_1} = \left[\langle (\phi^n_j)', (\phi^n_i)' \rangle_{\tilde{\omega}_1,(0,1)}\right]^{n-1}_{i,j=0} \quad \text{with} \quad \tilde{\omega}_1(x) = \frac{1}{x \log|2x| \log^{\chi}\log|2x|}.$$

Then, one easily concludes that

$$K^{\phi}_{\omega_1} \preceq \log n \log^{\chi}\log n \; K^{\phi}_{\tilde{\omega}_1}.$$

Now, we are able to apply Theorem 3.6 and obtain the desired result as in the proof of Theorem 3.7. □

3.2.2 First numerical experiments

The purpose of this subsection is to present first numerical experiments concerning the quality of the preconditioners C_M^{-1} (3.20) and C_K^{-1} (3.22) for the matrices $K^{\tilde{L}_{(-1,1)}}$ (3.7) and $M^{\tilde{L}_{(-1,1)}}$ (3.6), respectively. Our wavelet preconditioners are developed for the interval $(0,1)$, whereas the interpretations of $M^{\tilde{L}_{(-1,1)}}$ and $K^{\tilde{L}_{(-1,1)}}$ are given for the interval $(-1,1)$, cf. Lemmas 3.1 and 3.2. Therefore, we have to adapt the matrices $M^{\tilde{L}_{(-1,1)}}$ and $K^{\tilde{L}_{(-1,1)}}$, cf. Remark 3.4. This means that we first test our preconditioners only to the matrices $K^{\tilde{L}_{(-1,1)}}_{even}$ and $M^{\tilde{L}_{(-1,1)}}_{even}$.
In all experiments, we choose the family of wavelets which is generated by the wavelet ψ_{22}. This wavelet consists of two vanishing moments on the primal and the dual side. Figure 2 depicts a picture of ψ_{22} and its dual function.

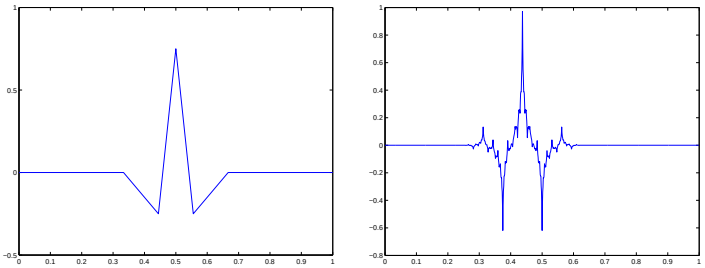

Figure 2: Plot of wavelet ψ_{22} (left) and its dual $\tilde{\psi}_{22}$ (right)

The maximal and minimal eigenvalue of $C_K^{-1} M^{\tilde{L}_{(-1,1)}}_{even}$ and $C_M^{-1} K^{\tilde{L}_{(-1,1)}}_{even}$ are displayed in Figure 3. In both experiments, we have replaced the diagonal matrices D_M and D_K in (3.20) and (3.22) by the diagonal parts of

$$Q_k^{\top} K^{\tilde{L}_{(-1,1)}}_{even} Q_k \quad \text{and} \quad Q_k^{\top} M^{\tilde{L}_{(-1,1)}}_{even} Q_k.$$

This is the best possible choice of a diagonal matrix. From the experiments, a moderate dependence of the eigenvalue bounds from the polynomial degree p can be seen. However, three of the four eigenvalue bounds are quite far away from one.

3.2.3 Improvement of the constants by a block diagonal scaling

As we have observed in the previous subsection, the constants are too large. The reasons are the diagonal scaling for the coarse grid problem on level 0 (Neumann problem) and the difficulties

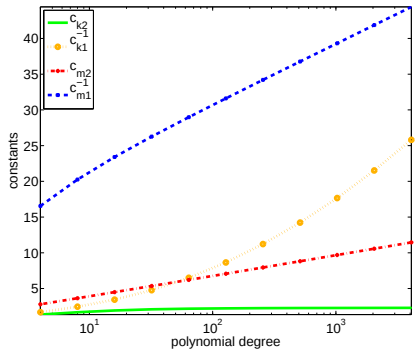

Figure 3: Maximal and minimal eigenvalue of $C_K^{-1} M_{even}^{\tilde{L}_{(-1,1)}}$ (constants $c_{k,1}$ and $c_{k,2}$) and $C_M^{-1} K_{even}^{\tilde{L}_{(-1,1)}}$ (constants $c_{m,1}$ and $c_{m,2}$).

with the weight function at the singular boundary. In order to reduce the constants, we use an idea which has been proposed in [6] for a similar problem. We replace the diagonal matrices D_M and D_K in (3.20) and (3.22) by block diagonal matrices. For all wavelets ψ_j^l with $\psi_j^l(0) \neq 0$, i.e. with $j \geq 1$, we use again a diagonal scaling with respect to the wavelet basis. For the boundary wavelets, i.e. wavelets with $\psi_j^l(0) \neq 0$ or $j = 0$, the corresponding block is inverted exactly. The size of the block is about $k = \log_2 n$, i.e. it is small in comparison to the original matrix. More precisely, the matrix D_M in (3.20) is replaced by the matrix

$$(\tilde{D}_M)_{(j,l),(j',l')} = \begin{cases} M^{\psi}_{l,l'} & j = j' = 0 \\ (D_M)_{(j,l),(j',l')} & \text{else} \end{cases} \quad \text{with} \quad M^{\psi}_{l,l'} = \int_0^1 x \psi_0^l \psi_0^{l'} \, \mathrm{d}x \tag{3.24}$$

and the matrix D_K in (3.22) is replaced by the matrix

$$(\tilde{D}_K)_{(j,l),(j',l')} = \begin{cases} K^{\psi}_{l,l'} & j = j' = 0 \\ (D_K)_{(j,l),(j',l')} & \text{else} \end{cases} \quad \text{with} \quad K^{\psi}_{l,l'} = \int_0^1 \omega_1^2(x) (\psi_0^l)'(\psi_0^{l'})' \, \mathrm{d}x. \tag{3.25}$$

Figure 4 shows that this approach reduces the eigenvalue bounds dramatically. Now, all eigenvalue bounds are close to 1. For the relevant computational range up to a maximal polynomial degree of $p = 31$, all constants are essentially bounded by 2.
In a next step, we develop the preconditioners for the matrices $K^{\phi}_{\omega_1}$ (3.16) and $M^{\phi}_{\omega_2}$ (3.12) on the interval $(-1, 1)$. Now, the singularities of the weight function lie in the interior of the interval at $x = 0$. Again, we intend to use a wavelet preconditioner. As we have observed from the previous examples, see Figures 3 and 4, the main difficulty is the coupling between wavelets with $\psi_j^l(0) = 0$. Hence, we propose preconditioners of the form

$$\mathcal{C}_K^{-1} = \mathcal{Q}_k (\mathcal{D}_K)^{-1} \mathcal{Q}_k^{\top} \quad \text{and} \quad \mathcal{C}_M^{-1} = \mathcal{Q}_k (\mathcal{D}_M)^{-1} \mathcal{Q}_k^{\top} \tag{3.26}$$

for $K^{\phi}_{\omega_1}$ (3.16) and $M^{\phi}_{\omega_2}$ (3.12), respectively, where $\mathcal{Q}_k$ denotes the corresponding wavelet transformation matrix from the basis $[\Phi_n^1]$ to the wavelet basis $[\Psi_k]$, cf. (3.17). The matrices $\mathcal{D}_M$ and

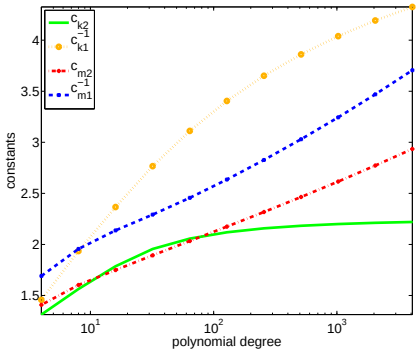

Figure 4: Maximal and minimal eigenvalue of $C_K^{-1}M_{1,even}$ (constants $c_{k,1}$ and $c_{k,2}$) and $C_M^{-1}K_{1,even}$ (constants $c_{m,1}$ and $c_{m,2}$) with block diagonal scaling.

$\mathcal{D}_K$ are defined as

$$(\mathcal{D}_M)_{(j,l),(j',l')} = \begin{cases} \mathcal{M}^{\psi}_{l,l'} & j=j'=0 \\ \delta_{jj'}\delta_{ll'}\omega_2^2(2^{-l}j) & \text{else} \end{cases} \quad \text{with} \quad \mathcal{M}^{\psi}_{l,l'} = \int_{-1}^{1} x\psi_0^l\psi_0^{l'}\,\mathrm{d}x, \tag{3.27}$$

$$(\mathcal{D}_K)_{(j,l),(j',l')} = \begin{cases} \mathcal{K}^{\psi}_{l,l'} & j=j'=0 \\ \delta_{jj'}\delta_{ll'}2^{2l}\omega_1^2(2^{-l}j) & \text{else} \end{cases} \tag{3.28}$$

$$\text{with} \quad \mathcal{K}^{\psi}_{l,l'} = \int_{-1}^{1} \omega_1^2(x)(\psi_0^l)'(\psi_0^{l'})'\,\mathrm{d}x,$$

where δ_{ij} denotes the Kronecker delta. This is similar to (3.24), (3.25).
Due to Lemmas 3.1 and 3.2, the preconditioners $\mathcal{C}_K$ and $\mathcal{C}_M$ (3.26) can also be used as preconditioners for $M^{\tilde{L}_{(-1,1)}}$ (3.6) and $K^{\tilde{L}_{(-1,1)}}$ (3.7), respectively. Using Lemma 3.1 and Theorem 3.7, we obtain

$$\frac{p^2}{\log p \log^{\chi}\log p}\mathcal{C}_M \preceq K^{\tilde{L}_{(-1,1)}} \preceq p^2\mathcal{C}_M \tag{3.29}$$

with $n = \frac{p+1}{2}$. By Lemma 3.2 and Theorem 3.8, one can conclude that

$$\mathcal{C}_K \preceq p^2 M^{\tilde{L}_{(-1,1)}} \preceq \log p \log^{\chi}\log p\, \mathcal{C}_K \quad \text{with } \chi > 1. \tag{3.30}$$

A direct consequence of the definition of the preconditioners in (3.26) and relations (3.29), (3.30) is the following result about the stability of the basis

$$[\Psi_{pol,p,[-1,1]}] = [\tilde{L}_{(-1,1)}]\mathcal{Q}_k \tag{3.31}$$

in $L_2(-1,1)$ and $H^1(-1,1)$.

Lemma 3.9. *Let $[\Psi_{pol,p,[-1,1]}]$ be defined via (3.31). Then, there exist two blockdiagonal matrices $D^{\psi}_M = \text{blockdiag}\left[D^{\psi}_{M,1}, D^{\psi}_{M,2}\right]$ and $D^{\psi}_K = \text{blockdiag}\left[D^{\psi}_{K,1}, D^{\psi}_{K,2}\right]$ which have the following properties*

- *The matrices $D^{\psi}_{K,1} \in \mathbb{R}^{m,m}$ and $D^{\psi}_{M,1} \in \mathbb{R}^{m,m}$ are dense where $m \approx \log_2 p$.*
- *The matrices $D^{\psi}_{K,2}$ and $D^{\psi}_{M,2}$ are diagonal.*

Moreover, for any $u = \left[\Psi_{pol,p,[-1,1]}\right] \underline{u}$*, we have*

$$\left(D_M^{\psi}\underline{u},\underline{u}\right) \preceq \quad \| u \|^2_{L_2(-1,1)} \quad \preceq \log p \log^{\chi} \log p \left(D_M^{\psi}\underline{u},\underline{u}\right), \tag{3.32}$$

$$\frac{1}{\log p \log^{\chi} \log p}\left(D_K^{\psi}\underline{u},\underline{u}\right) \preceq \quad |u|^2_{H_1(-1,1)} \quad \preceq \left(D_K^{\psi}\underline{u},\underline{u}\right) \tag{3.33}$$

for any $\chi > 1$*.*

3.3 Wavelets solvers on two elements

3.3.1 Extension to neighboring elements

In the previous subsection, quasioptimal solvers for $K^{\tilde{L}_{(-1,1)}}$ and $M^{\tilde{L}_{(-1,1)}}$ have been developed. Now, we have to consider the preconditioners for the assembled matrices $M^{\tilde{L}_{(-2,2)}}$ and $K^{\tilde{L}_{(-2,2)}}$. Therefore, we have to investigate the extension of the functions (3.31) to the neightbouring element. We consider now the model problem (2.3) with two elements $(-2,0)$ and $(0,2)$. In the basis of the integrated Legendre polynomials, see (3.5), only the hat function is nonzero at $x = 0$. In the previous subsection, we have transformed all basis functions on one element locally to another basis $[\Psi_{pol,p,[-1,1]}]$ (3.31). Let $[\Psi_{pol,p,[0,2]}] = [\psi_{pol,i}]_{i=0}^{p-1}$ be the similar functions on $[0,2]$ under the affine transformation $y = x + 1$, i.e. $[\Psi_{pol,p,[0,2]}] = [\Psi_{pol,p,[-1,1]}] \circ (\cdot + 1)$. Due to the definition of the matrix $\mathcal{Q}_k$, about $m + 1 \approx \log_2 p$ functions of $\Psi_{pol,p,[0,2]}$ are nonzero at $x = 0$. Without loss of generality let us assume that

$$\psi_{pol,i}(0) \neq 0 \ \leftrightarrow \ i = 0, \ldots, m.$$

None of these functions can continuously be extended by 0 to the neighboring element $[-2,0]$. Let $\psi_{pol,0}$ be the function which corresponds to the wavelet ψ_0^0 (coarse hat-function). Then, we define

$$\tilde{\psi}_{p,j}(x) \quad = \quad \begin{cases} \begin{cases} \psi_{pol,j}(x) & x \in [0,2] \\ \frac{\psi_{pol,j}(0)}{\psi_{pol,0}(0)}\psi_{pol,0}(-x) & x \in [-2,0] \end{cases} & j = 0, \ldots, p-1 \\ \begin{cases} \psi_{pol,j}(-x) & x \in [-2,0] \\ \frac{\psi_{pol,j}(0)}{\psi_{pol,0}(0)}\psi_{pol,0}(x) & x \in [0,2] \end{cases} & j = 1-p, \ldots, -1 \end{cases}. \tag{3.34}$$

Note that $\tilde{\psi}_{p,j}(x) \mid_{(-2,0)} = 0$ if $j \geq m$. Moreover, let

$$[\tilde{\Psi}_p] = \left[\tilde{\psi}_{p,j}\right]_{j=-p+1}^{p-1} \tag{3.35}$$

denote corresponding vector of basis functions. We now have to prove the linear independence of the functions $\tilde{\psi}_{p,j}$. Moreover, a stability result as in (3.32), (3.33) is required. Therefore, two theoretical results have to be shown.

Lemma 3.10. *Assume that* $\alpha \neq 0$*,* $\underline{q}, \underline{r} \in \mathbb{R}^{n\times 1}$ *and* $W \in \mathbb{R}^{n\times n}$*. Moreover, let* $\begin{bmatrix} \alpha & \underline{r}^{\top} \\ \underline{q} & W \end{bmatrix}$ *be nonsingular. Then, the matrix*

$$W_g = \begin{bmatrix} W & \underline{q} & \alpha^{-1}\underline{q}\underline{r}^{\top} \\ \underline{r}^{\top} & \alpha & \underline{r}^{\top} \\ \alpha^{-1}\underline{q}\underline{r}^{\top} & \underline{q} & W \end{bmatrix}$$

is nonsingular.

Proof. We prove that $\ker W_g = \underline{0}$. According to the partition of W_g, we set $\underline{x} = \begin{bmatrix} \underline{x}_- \\ x_0 \\ \underline{x}_+ \end{bmatrix}$. The relation $W_g\underline{x} = \underline{0}$ implies the equations

$$\begin{aligned} \underline{r}^\top \underline{x}_- + \alpha x_0 + \underline{r}^\top \underline{x}_+ &= 0, \\ W\underline{x}_- + \underline{q}x_0 + \alpha^{-1}\underline{q}\underline{r}^\top \underline{x}_+ &= 0, \quad \text{and} \\ \alpha^{-1}\underline{q}\underline{r}^\top \underline{x}_- + \underline{q}x_0 + W\underline{x}_+ &= 0. \end{aligned}$$

Multiplying the first equation by $\alpha^{-1}\underline{q}$ and subtracting this from the second and the third equation gives

$$(W - \alpha^{-1}\underline{q}\underline{r}^\top)\underline{x}_+ = (W - \alpha^{-1}\underline{q}\underline{r}^\top)\underline{x}_- = \underline{0}.$$

Since the matrix $\begin{bmatrix} \alpha & \underline{r}^\top \\ \underline{q} & W \end{bmatrix}$ is nonsingular, the Schur complement $(W - \alpha^{-1}\underline{q}\underline{r}^\top)$ is nonsingular, too. This gives $\underline{x}_+ = \underline{x}_- = \underline{0}$. With $\alpha \neq 0$, we have $x_0 = 0$. This proves the assertion. □

The second lemma is similar to a result on assembled matrices, [30].

Lemma 3.11. *Let $[\Psi] = [\psi_i]_{i=-n}^{n}$ be a basis of continuous functions on the interval $I = (a_1, a_3)$. Moreover, let $I_1 = (a_1, a_2)$ and $I_2 = (a_2, a_3)$ with $a_1 < a_2 < a_3$. Let us assume that the basis $[\Psi]$ satisfies the following properties:*

1. *There exists an integer m with $0 < m < n$ such that*

$$\psi_i(x) \mid_{I_2} = 0 \quad \forall i > m \quad \text{and } \psi_i(x) \mid_{I_1} = 0 \quad \forall x \in I_1, i < -m. \tag{3.36}$$

   Moreover, there exist real numbers $\alpha_i \in \mathbb{R}$ such that

$$\psi_i(x) \mid_{I_2} = \alpha_i \psi_0(x) \quad \forall i = 1, \ldots, m \quad \text{and } \psi_i(x) \mid_{I_1} = \alpha_i \psi_0(x) \quad \forall -i = 1, \ldots, m. \tag{3.37}$$

2. *For $j = 1, 2$, let $D_j = \begin{bmatrix} D_{j,1} & \mathbf{0} \\ \mathbf{0} & D_{j,2} \end{bmatrix} \in \mathbb{R}^{n+1 \times n+1}$, where $D_{j,1} \in \mathbb{R}^{m+1 \times m+1}$ and $D_{j,2}$ are diagonal matrices. Let $\| \cdot \|_I$ be some norm of a function space of functions $f : I \mapsto \mathbb{R}$ which is induced by a scalar product $(\cdot, \cdot)_I$. Moreover, let us assume that the estimates*

$$\begin{aligned} c_1^{-1}\underline{u}_1^\top D_1 \underline{u}_1 &\leq \| u_1 \|_{I_1}^2 \leq c_2 \underline{u}_1^\top D_1 \underline{u}_1 \\ c_1^{-1}\underline{u}_2^\top D_2 \underline{u}_2 &\leq \| u_2 \|_{I_2}^2 \leq c_2 \underline{u}_2^\top D_2 \underline{u}_2 \end{aligned} \tag{3.38}$$

   are valid for any $u_1 = [\psi_i]_{i=0}^{n} \underline{u}_1$ and any $u_2 = [\psi_{-i}]_{i=0}^{n} \underline{u}_2$ where c_1 and c_2 denote some constants.

Then the estimates

$$c_1^{-1}\underline{u}^\top D \underline{u} \leq \| u \|_I^2 \leq c_2 \underline{u}^\top D \underline{u}$$

hold for any $u = [\Psi]\underline{u}$, where

$$D = \begin{bmatrix} D_{2,2} & \mathbf{0} & \mathbf{0} \\ \mathbf{0} & R & \mathbf{0} \\ \mathbf{0} & \mathbf{0} & D_{1,2} \end{bmatrix}$$

with some matrix $R \in \mathbb{R}^{2m+1 \times 2m+1}$.

Proof. We have

$$\begin{aligned}
\| u \|_I^2 = \| [\Psi]\underline{u} \|_I^2 &= \| \sum_{i=-n}^{n} u_i\psi_i \|_I^2 \\
&= \| \sum_{i=-n}^{n} u_i\psi_i \|_{I_1}^2 + \| \sum_{i=-n}^{n} u_i\psi_i \|_{I_2}^2 \\
&= \| \sum_{i=-m}^{n} u_i\psi_i \|_{I_1}^2 + \| \sum_{i=-n}^{m} u_i\psi_i \|_{I_2}^2 \\
&= \| \tilde{u}_0\psi_0 + \sum_{i=1}^{n} u_i\psi_i \|_{I_1}^2 + \| \hat{u}_0\psi_0 + \sum_{i=-n}^{-1} u_i\psi_i \|_{I_2}^2
\end{aligned}$$

by (3.36) and (3.37) with $\tilde{u}_0 = u_0 + \sum_{i=-m}^{-1} u_i\alpha_i$ and $\hat{u}_0 = u_0 + \sum_{i=1}^{m} u_i\alpha_i$. Let $\underline{u}_+ = [u_i]_{i=m+1}^{n}$, $\underline{u}_- = [u_i]_{i=-n}^{-m-1}$, $\underline{u}_0 = [u_i]_{i=-m}^{m}$. Using (3.38), we can conclude that

$$\begin{aligned}
c_2^{-1}(\| u \|_{I_1}^2 + \| u \|_{I_2}^2) &\le \begin{bmatrix} \underline{u}_- \\ \underline{u}_0 \\ \underline{u}_+ \end{bmatrix}^\top \begin{bmatrix} \mathbf{0} & \mathbf{0} & \mathbf{0} \\ \mathbf{0} & R_1 & \mathbf{0} \\ \mathbf{0} & \mathbf{0} & D_{1,2} \end{bmatrix} \begin{bmatrix} \underline{u}_- \\ \underline{u}_0 \\ \underline{u}_+ \end{bmatrix} \\
&\quad + \begin{bmatrix} \underline{u}_- \\ \underline{u}_0 \\ \underline{u}_+ \end{bmatrix}^\top \begin{bmatrix} D_{2,2} & \mathbf{0} & \mathbf{0} \\ \mathbf{0} & R_2 & \mathbf{0} \\ \mathbf{0} & \mathbf{0} & \mathbf{0} \end{bmatrix} \begin{bmatrix} \underline{u}_- \\ \underline{u}_0 \\ \underline{u}_+ \end{bmatrix} \\
&= \begin{bmatrix} \underline{u}_- \\ \underline{u}_0 \\ \underline{u}_+ \end{bmatrix}^\top \begin{bmatrix} D_{2,2} & \mathbf{0} & \mathbf{0} \\ \mathbf{0} & R & \mathbf{0} \\ \mathbf{0} & \mathbf{0} & D_{1,2} \end{bmatrix} \begin{bmatrix} \underline{u}_- \\ \underline{u}_0 \\ \underline{u}_+ \end{bmatrix}
\end{aligned}$$

with some symmetric and positive definite matrices $R_j \in \mathbb{R}^{2m+1\times 2m+1}$, $j = 1, 2$ and $R = R_1 + R_2$. This proves the upper estimate. The lower estimate can be proved in the same way. □

Now, we are able to return to the basis $[\tilde{\Psi}_p]$ and introduce the sparse matrices

$$\begin{aligned}
(\tilde{\mathfrak{D}}_M)_{ij} &= \left\{ \begin{array}{cc} \int_{-2}^{2} \tilde{\psi}_i(x)\tilde{\psi}_j(x)\,\mathrm{d}x & |i|,|j| \le m \\ \int_{-2}^{2} \tilde{\psi}_i(x)\tilde{\psi}_j(x)\,\mathrm{d}x \cdot \delta_{ij} & \text{else} \end{array} \right\} \quad \text{and} \qquad (3.39) \\
(\tilde{\mathfrak{D}}_K)_{ij} &= \left\{ \begin{array}{cc} \int_{-2}^{2} \tilde{\psi}_i'(x)\tilde{\psi}_j'(x)\,\mathrm{d}x & |i|,|j| \le m \\ \int_{-2}^{2} \tilde{\psi}_i(x)\tilde{\psi}_j(x)\,\mathrm{d}x \cdot \delta_{ij} & \text{else} \end{array} \right\}.
\end{aligned}$$

Lemma 3.12. *Let $[\tilde{\Psi}_p]$ be defined via (3.35) and let $\tilde{\mathfrak{D}}_M$ and $\tilde{\mathfrak{D}}_K$ be defined via (3.39). Then the functions $\tilde{\psi}_i$ are linearly independent. Moreover, the relations*

$$c_{M,1}^{-1}\left(\tilde{\mathfrak{D}}_M\underline{u},\underline{u}\right) \le \| u \|_{L_2(-2,2)}^2 \le c_{M,2}\left(\tilde{\mathfrak{D}}_M\underline{u},\underline{u}\right), \qquad (3.40)$$

and

$$c_{K,1}^{-1}\left(\tilde{\mathfrak{D}}_K\underline{u},\underline{u}\right) \le \| u \|_{H^1(-2,2)}^2 \le c_{K,2}\left(\tilde{\mathfrak{D}}_K\underline{u},\underline{u}\right) \qquad (3.41)$$

hold for any $u = [\tilde{\Psi}_p]\underline{u} \in \mathbb{B}_p$. The constants $c_{M,1}$ and $c_{K,2}$ are independent of the polynomial degree p, whereas $c_{M,2} = c_{K,1} = \mathcal{O}(\log p \log^\chi \log p)$ with some $\chi > 1$.

Proof. Due to the construction of our basis functions in (3.34), the assumptions of Lemmas 3.10 and 3.11 are satisfied. The linear independence of the basis functions follows from Lemma 3.10. For the proof of (3.40), we use Lemma 3.10 with $\|\cdot\|_I = \|\cdot\|_{L_2(-2,2)}$. The definition (3.34) implies the assumptions (3.36) and (3.37). Inequality (3.30) implies relation (3.38) with $c_1 = \mathcal{O}(1)$ and $c_2 = \mathcal{O}(\log p \log^\chi \log p)$. This proves (3.40). For (3.41), we use Lemma 3.10 again with $\|\cdot\|_I = \|\cdot\|_{H^1(-2,2)}$ and relation (3.29). □

Relation (3.39) implies that the matrices $\tilde{\mathfrak{D}}_K$ and $\tilde{\mathfrak{D}}_M$ are block-diagonal matrices, i.e

$$\tilde{\mathfrak{D}}_M = \begin{bmatrix} \mathfrak{D}_{M,-} & \mathbf{0} & \mathbf{0} \\ \mathbf{0} & \mathfrak{M} & \mathbf{0} \\ \mathbf{0} & \mathbf{0} & \mathfrak{D}_{M,+} \end{bmatrix} \quad \text{and} \quad \tilde{\mathfrak{D}}_K = \begin{bmatrix} \mathfrak{D}_{K,-} & \mathbf{0} & \mathbf{0} \\ \mathbf{0} & \mathfrak{K} & \mathbf{0} \\ \mathbf{0} & \mathbf{0} & \mathfrak{D}_{K,+} \end{bmatrix} \tag{3.42}$$

where $\mathfrak{D}_{M/K,+/-} \in \mathbb{R}^{n-m \times n-m}$ are diagonal matrices. Therefore block-diagonal matrices $\tilde{\mathfrak{D}}_M$ and $\tilde{\mathfrak{D}}_K$ are required in order to prove the stability results (3.40) and (3.41), respectively. In order to prove similar results with diagonal matrices $\mathfrak{D}_K$ and $\mathfrak{D}_M$, the basis functions $\tilde{\psi}_i$, $-m \leq i \leq m$, have to be modified. Therefore, we consider the generalized eigenvalue problem

$$\mathfrak{K}\underline{x} = \lambda \mathfrak{M}\underline{x}. \tag{3.43}$$

Let G and Λ be the matrix of the eigenvectors and the diagonal matrix of the eigenvalues, respectively, i.e.

$$G^\top \mathfrak{K} G = \Lambda \quad \text{and} \quad G^\top \mathfrak{M} G = I. \tag{3.44}$$

Moreover, let

$$[\psi_{p,i}]_{i=-m}^{m} = [\tilde{\psi}_{p,i}]_{i=-m}^{m} G, \;\; \psi_{p,i}(x) = \tilde{\psi}_{p,i}(x), \; |i| \geq m, \quad \text{and} \quad [\Psi_p] = [\psi_{p,i}]_{i=-p+1}^{p-1}. \tag{3.45}$$

The basis transformation between the basis $[\Psi_p]$ (3.45) and the basis of the integrated Legendre polynomials $[\tilde{L}_{(-2,2)}]$ (3.3) is expressed via

$$[\Psi_p] = [\tilde{L}_{(-2,2)}] W_p \tag{3.46}$$

where $W_p \in \mathbb{R}^{2p-1 \times 2p-1}$ is a nonsingular matrix. Finally, we introduce the diagonal matrices

$$\mathfrak{D}_M = \begin{bmatrix} \mathfrak{D}_{M,-} & \mathbf{0} & \mathbf{0} \\ \mathbf{0} & I & \mathbf{0} \\ \mathbf{0} & \mathbf{0} & \mathfrak{D}_{M,+} \end{bmatrix} \quad \text{and} \quad \mathfrak{D}_K = \begin{bmatrix} \mathfrak{D}_{K,-} & \mathbf{0} & \mathbf{0} \\ \mathbf{0} & \Lambda & \mathbf{0} \\ \mathbf{0} & \mathbf{0} & \mathfrak{D}_{K,+} \end{bmatrix} \tag{3.47}$$

with $\mathfrak{D}_{M/K,+/-} \in \mathbb{R}^{n-m \times n-m}$ of (3.42). Now, we are able to prove the following stability result for the basis $[\Psi_p]$.

Theorem 3.13. *Let $[\Psi_p]$, $\mathfrak{D}_M$ and $\mathfrak{D}_K$ be defined via (3.45) and (3.47), respectively. Then the relations*

$$c_{m,1}^{-1} \left(\mathfrak{D}_M \underline{u}, \underline{u}\right) \leq \| u \|_{L_2(-2,2)}^2 \leq c_{m,2} \left(\mathfrak{D}_M \underline{u}, \underline{u}\right), \tag{3.48}$$

and

$$c_{k,1}^{-1} \left(\mathfrak{D}_K \underline{u}, \underline{u}\right) \leq \| u \|_{H^1(-2,2)}^2 \leq c_{k,2} \left(\mathfrak{D}_K \underline{u}, \underline{u}\right) \tag{3.49}$$

hold for any $u = [\Psi_p]\underline{u} \in \mathbb{B}_p$. The constants $c_{m,1}$, $c_{k,2}$, $c_{m,2}$ and $c_{k,1}$ are the constants of (3.40) and (3.41), i.e. $c_{m,2} = c_{k,1} = \mathcal{O}(\log p \log^\chi \log p)$ with some $\chi > 1$, whereas $c_{m,1}$ and $c_{k,2}$ are independent of p. Moreover, the operations $W_p \underline{x}$ and $W_p^\top \underline{x}$ require $\mathcal{O}(p)$ floating point operations.

Proof. The assertions (3.48) and (3.49) are direct consequences of (3.40) and (3.41) using (3.47) and (3.44). The basis transformation matrix W_p (3.46) involves two basis transformations:

- the wavelet transformation,
- the eigenvalue basis transformation (3.44).

The first one is preformed in $\mathcal{O}(p)$ operations. The second one requires the solution of a eigenvalue problem of size $2m+1$, where $m \approx \log_2 p$. Hence, the solution of (3.43) requires $\mathcal{O}(\log_2^3 p)$ flops, a multiplication with the matrix G requires $\mathcal{O}(\log_2^2 p)$ flops. Therefore, the total cost is $\mathcal{O}(p)$. □

3.3.2 Refinements for general p

In subsection 3.2, we have assumed that $n = 2^k$ and $n = \frac{p+1}{2}$. Therefore, the norm equivalences in Theorem 3.12 are only valid for $p = 2^k - 1$, i.e. for $p = 3, 7, 15, \ldots$. However, in order to develop a solver, we need also a similar result for general p. In order to define a preconditioner there, a wavelet transformation and refinement strategy for general $n \neq 2^k$ is required. Here, we use a two level argument. Let $k = [\log_2 n]$ be the largest integer of $[\log_2 n]$ which is not greater than $[\log_2 n]$ and set $n_0 = 2^{k_0}$. In a first step, we do now a symbolic refinement from n grid points to n_0 grid points. For the remaining n_0 grid points, we can now apply our wavelet transformation. The question arises, where the local refinement has to be done. Three possibilities are proposed:

`v1` local refinement at the nonsingular boundaries $x = \pm 1$,

`v2` by an averaging argument, i.e. the nodes $\pm[\frac{j\,n}{n-n_0}]$, $j = 1, \ldots, n - n_0$ are the new nodes on level $k_0 + 1$,

`v3` local refinement at the singularity $x = 0$,

cf. also Figure 5. For the two-level wavelet transformation from n to n_0, the wavelet ψ_{22} is used for `v1` and `v3` in the interior of the refinement. Otherwise, the wavelet ψ_{20} is used, see also Figure 5.

3.3.3 Numerical experiments

The first example considers the case $p = 2^k - 1$. In all experiments, the wavelet ψ_{22} is used for the refinement from n_0 to $\frac{n_0}{2}, \frac{n_0}{4}, \ldots$. Table 2 displays the constants $c_{m,r}$ and $c_{k,r}$, $r = 1, 2$, of the

p	3	7	15	31	63	127	255	511	1023
$c_{k,2}$	1.00	1.34	1.58	1.80	1.97	2.06	2.12	2.16	2.19
$c_{k,1}^{-1}$	1.00	1.51	2.00	2.41	2.79	3.12	3.41	3.65	3.86
$c_{m,2}$	1.00	1.40	1.59	1.74	1.88	2.03	2.17	2.31	2.46
$c_{m,1}^{-1}$	1.00	1.66	1.92	2.10	2.25	2.42	2.60	2.80	3.00

Table 2: Constants $c_{m,r}$ and $c_{k,r}$, $r = 1, 2$, of (3.40) and (3.41) for $p = 2^k - 1$.

norm equivalences (3.40), (3.41), respectively for different polynomial degrees. From the results it can be seen that all constants are very close to 1. Moreover, the constants are either uniformly bounded or increase logarithmically with respect to the polynomial degree p.
In the next experiment, we consider the quality of our wavelet transformation for general p. Figure 6 displays the results for the different versions `v1`, `v2` and `v3`. For all versions, the constants do depend only moderately on the polynomial degree p. The best results are obtained for `v3`, where the values are lower than for the next $p = 2^k - 1$.

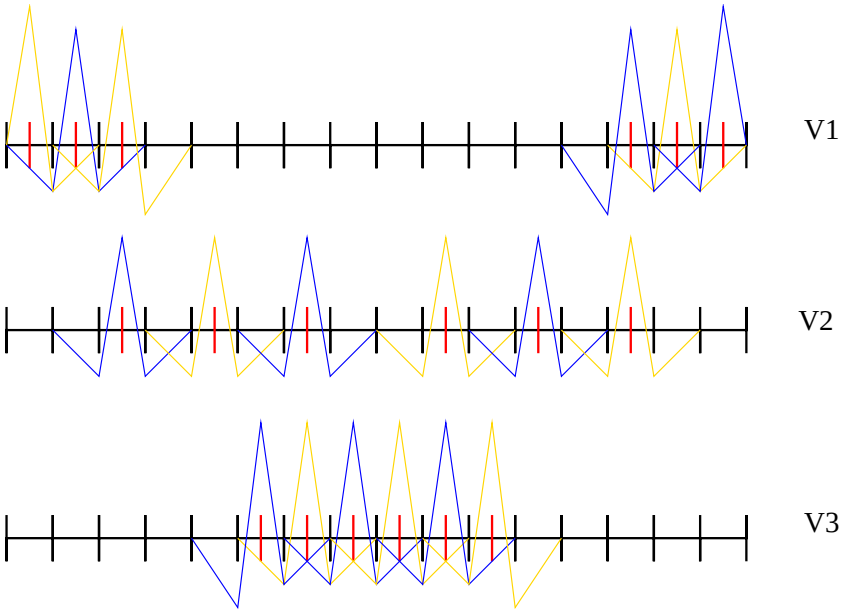

Figure 5: Refinement strategies for $p = 11$: `v3` (below), `v2` (middle) and `v1` (above). Fine nodes are marked red, coarse nodes are marked black, the wavelets are marked yellow or blue.

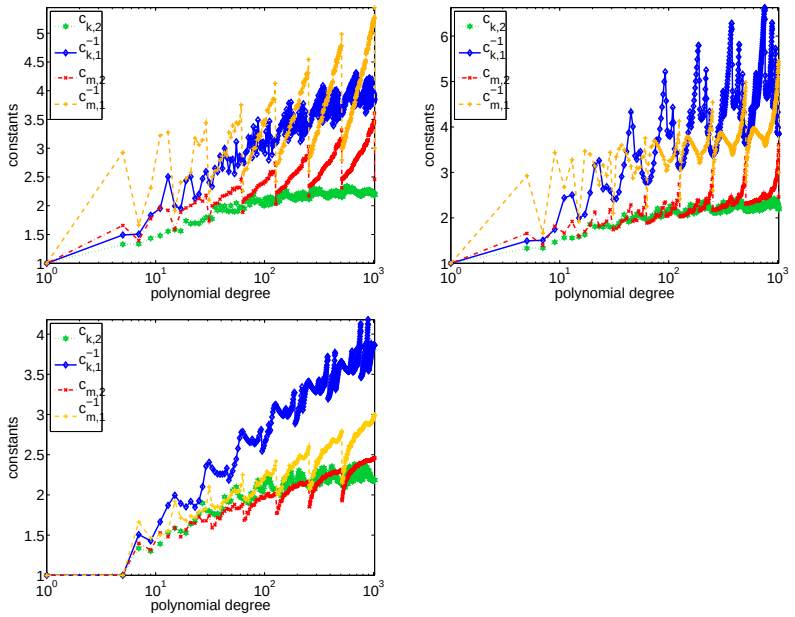

Figure 6: Constants $c_{m,r}$ and $c_{k,r}$, $r = 1, 2$, of (3.40) and (3.41) for general p, `v1` (above, left), `v2` (above, right), `v3` (below).

4 The 3D-solver

4.1 Condition number estimates

We are now in the position to define the wavelet solver for the three-dimensional model problem (2.5). Let W_p be defined via (3.46). Moreover, let $\mathfrak{D}_M$ and $\mathfrak{D}_K$ be defined via (3.47). Then, we introduce

$$C_3^{-1} = (W_p \otimes W_p \otimes W_p)(\mathfrak{D}_K \otimes \mathfrak{D}_M \otimes \mathfrak{D}_M + \mathfrak{D}_M \otimes \mathfrak{D}_K \otimes \mathfrak{D}_M + \mathfrak{D}_M \otimes \mathfrak{D}_M \otimes \mathfrak{D}_K)^{-1}(W_p \otimes W_p \otimes W_p)^\top. \quad (4.1)$$

Theorem 4.1. *Let C_3 and K_3 be defined via (4.1) and (2.5), respectively. Then we have the spectral estimate*

$$\frac{1}{\log p \log^\chi \log p} C_3 \preceq K_3 \preceq (\log p \log^\chi \log p)^2 C_3 \quad (4.2)$$

for any $\chi > 1$. Moreover, the operation $C_3^{-1}\underline{w}$ requires $\mathcal{O}(p^3)$ operations.

Proof. Using (2.5), we have

$$K_3 = K^{\tilde{L}_{(-2,2)}} \otimes M^{\tilde{L}_{(-2,2)}} \otimes M^{\tilde{L}_{(-2,2)}} + M^{\tilde{L}_{(-2,2)}} \otimes K^{\tilde{L}_{(-2,2)}} \otimes M^{\tilde{L}_{(-2,2)}} + M^{\tilde{L}_{(-2,2)}} \otimes M^{\tilde{L}_{(-2,2)}} \otimes K^{\tilde{L}_{(-2,2)}}.$$

By (3.48) and (3.49), one obtains

$$\begin{aligned} \mathfrak{D}_M &\preceq W_p^\top M^{\tilde{L}_{(-2,2)}} W_p \preceq \log p \log^\chi \log p \, \mathfrak{D}_M, \\ \frac{1}{\log p \log^\chi \log p} \mathfrak{D}_K &\preceq W_p^\top K^{\tilde{L}_{(-2,2)}} W_p \preceq \mathfrak{D}_K, \end{aligned}$$

respectively. These two inequalities are equivalent to

$$\begin{aligned} W_p^{-\top} \mathfrak{D}_M W_p^{-1} &\preceq M^{\tilde{L}_{(-2,2)}} \preceq \log p \log^\chi \log p \, W_p^{-\top} \mathfrak{D}_M W_p^{-1} \quad \text{and} \quad (4.3) \\ \frac{1}{\log p \log^\chi \log p} W_p^{-\top} \mathfrak{D}_K W_p^{-1} &\preceq K^{\tilde{L}_{(-2,2)}} \preceq W_p^{-\top} \mathfrak{D}_K W_p^{-1}. \end{aligned}$$

The assertion (4.2) follows now from (4.1) by the properties of the Kronecker product.
Since $\mathfrak{D}_M$ and $\mathfrak{D}_K$ (3.47) are diagonal matrices, the solution of

$$(\mathfrak{D}_K \otimes \mathfrak{D}_M \otimes \mathfrak{D}_M + \mathfrak{D}_M \otimes \mathfrak{D}_K \otimes \mathfrak{D}_M + \mathfrak{D}_M \otimes \mathfrak{D}_M \otimes \mathfrak{D}_K)^{-1}$$

requires $\mathcal{O}(p^3)$ operations. This proves the theorem. □

Remark 4.2. *The preconditioner C_3^{-1} is not robust for differential operators with an anisotropic diffusion matrix $\mathcal{A} = \mathrm{diag}[a_1, a_2, a_3]$ in (1.1). Instead of K_3 (2.5), the matrix*

$$\begin{aligned} \tilde{K}_3 \quad = \quad & a_1 K^{\tilde{L}_{(-2,2)}} \otimes M^{\tilde{L}_{(-2,2)}} \otimes M^{\tilde{L}_{(-2,2)}} \\ & + a_2 M^{\tilde{L}_{(-2,2)}} \otimes K^{\tilde{L}_{(-2,2)}} \otimes M^{\tilde{L}_{(-2,2)}} + a_3 M^{\tilde{L}_{(-2,2)}} \otimes M^{\tilde{L}_{(-2,2)}} \otimes K^{\tilde{L}_{(-2,2)}} \end{aligned}$$

has to be considered. Then, the matrix

$$\tilde{C}_3^{-1} = (W_p \otimes W_p \otimes W_p)(a_1 \mathfrak{D}_K \otimes \mathfrak{D}_M \otimes \mathfrak{D}_M + a_2 \mathfrak{D}_M \otimes \mathfrak{D}_K \otimes \mathfrak{D}_M + a_3 \mathfrak{D}_M \otimes \mathfrak{D}_M \otimes \mathfrak{D}_K)^{-1}(W_p \otimes W_p \otimes W_p)^\top.$$

is a quasioptimal and robust preconditioner for $\tilde{K}_3$. With an similar argument, anisotropies of the elements and the polynomial degree p can be handled, see [6].

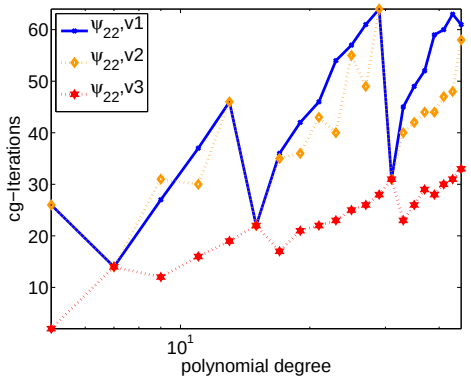

Figure 7: PCG-iterations for $K_3\underline{u} = \underline{f}$ using the preconditioner C_3 (4.1).

4.2 Numerical experiments

In this subsection, the system $K_3\underline{u} = \underline{f}$ is solved by a PCG-method with the preconditioner C_3^{-1} (4.1). In all experiments, the right hand side $\underline{f} = [1, \ldots, 1]^\top$ is chosen. The relative accuracy is 10^{-6}. Figure 7 displays the numbers of iterations for the polynomial degrees $p = 5, 7, 9, \ldots, 45$. In all experiments, a moderate increase of the iteration numbers can be observed for `v1`, `v2`, and `v3`. The preconditioner which uses the refinement strategy `v3`, needs about $15, \ldots, 30$ iterations, whereas the preconditioners with `v1` and `v2` need sometimes more than 50 iterations. Therefore the refinement strategy `v3` should be preferred.

4.3 Comparisons to direct solvers

In this subsection, the solution time of $K_3\underline{u} = \underline{f}$ by the PCG method with the preconditioner (4.1) is compared with sparse direct solvers. All experiments are performed on a Centrino 5, 1.6 GHz. The first experiment considers a comparison to a sparse Cholesky decomposition based on an approximate minimum degree permutation, [11]. The iterative solvers use a p-dependent relative accuracy of $10^{-5-p/3}$ in order to simulate the exponential convergence order of the hp-version of the FEM. Figure 8 displays the solution time for $p = 3, 5, \ldots, 15$. Note that the wavelet preconditioner

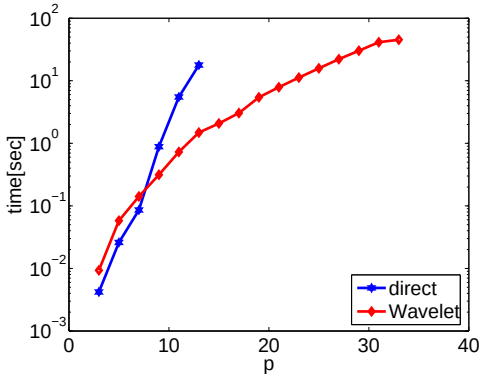

Figure 8: Comparison PCG-method with wavelet preconditioner vs. sparse direct solver

C_3^{-1} (4.1) is the exact solver for $p = 3$ and $p = 5$. For $p = 7$, the direct solver is faster than the

iterative solver. For $p \geq 9$, the iterative solver outperforms the direct solver.

5 Conclusions and Outlook

We have presented a solver for the system of linear equations arising from the discretization of $2 \times 2 \times 2$ cubes by means of the p-version of the FEM. This solver is embedded in an overlapping preconditioner [23]. The total solver time is $\mathcal{O}(p^3 \log^{3/2} p (\log^{\chi} \log p)^{3/2})$ with some $\chi > 1$. The solver can be applied to any situation of $2 \times 2 \times 2$ elements. This solver is also robust with respect to anisotropies which have their origin in the differential operator or the structure of the elements. In general, some vertex patches will not have the topological structure of $2 \times 2 \times 2$ elements. However, the ideas presented in the paper using the generalization of Theorem 3.13 simplify the development of difficult to implement nonoverlapping domain decomposition preconditioners with extension operators. More precisely, the wavelet construction helps to develop optimal and fast extension operators acting from the boundary of the elements to the interior and from the face boundaries to the faces.

A Basis functions and matrices

In Appendix A, we present the plots of the considered basis functions. The plots of the functions in the basis $[\Phi_3]$ are displayed in Figure 9. The plots of the functions $[\Psi_{31}]$ in (-2,0) are displayed

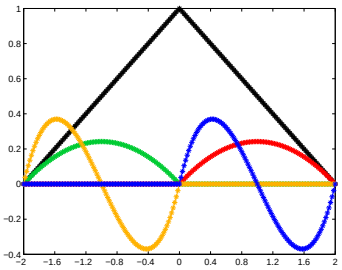

Figure 9: Integrated Legendre polynomials as basis functions of $\mathbb{B}_3$.

in Figure 10. The functions are enumerated in the following way:

- Firstly the function ψ_0 corresponding to the hierarchical functions,
- then the functions $\psi_1^b, \ldots, \psi_8^b$ with $\psi_j^b(0) \neq 0$ (2 per level, i.e. in total 8),
- the functions ψ_9^i and ψ_{10}^i with $\psi_j^i(0) = 0$ corresponding to level 1,
- the functions $\psi_{11}^i, \ldots, \psi_{16}^i$ with $\psi_j^i(0) = 0$ corresponding to level 2,
- and finally the functions $\psi_{17}, \ldots, \psi_{30}$ with $\psi_j(0) = 0$ corresponding to the fine level.

Moreover, we present the structure of the matrices K_p and M_p (2.4) for $p = 7$. The functions are ordered in the following way:

- Firstly, the hat function,
- the even polynomials of the first element $(-2, 0)$,

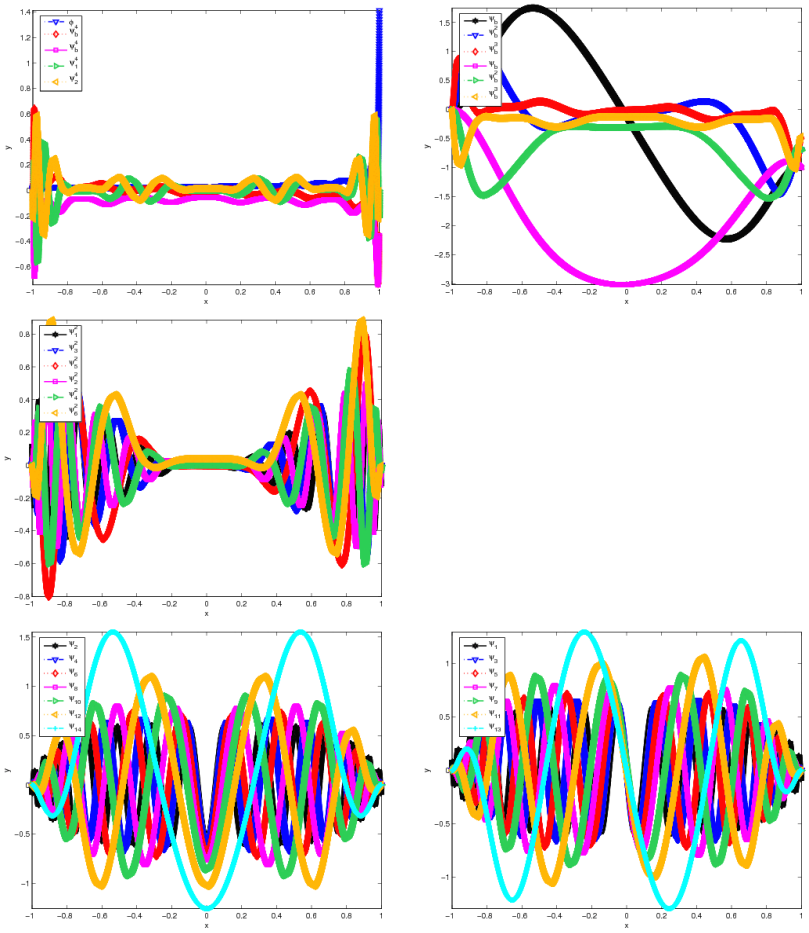

Figure 10: Plots of the functions of $[\Psi_{31}]$ on $(-2, 0)$.

- the odd polynomials of the first element $(-2, 0)$,
- the even polynomials of the second element $(0, 2)$,
- and finally the odd polynomials of the second element $(0, 2)$.

The polynomials are ordered in increasing order. In this basis, one easily concludes

$$K^{\tilde{L}_{(-2,2)}} = \frac{1}{4}\mathrm{diag}\left[4, 6, 14, 22, 10, 18, 26, 6, 14, 22, 10, 18, 22\right]. \tag{A.1}$$

Moreover, a simple computation shows that

$$M^{\tilde{L}_{(-2,2)}} = \frac{1}{4}\begin{bmatrix} \frac{16}{3} & \underline{a}_1^\top & \underline{a}_2^\top & \underline{a}_1^\top & \underline{a}_2^\top \\ \underline{a}_1 & B_1 & \mathbf{0} & \mathbf{0} & \mathbf{0} \\ \underline{a}_2 & \mathbf{0} & B_2 & \mathbf{0} & \mathbf{0} \\ \underline{a}_1 & \mathbf{0} & \mathbf{0} & B_1 & \mathbf{0} \\ \underline{a}_2 & \mathbf{0} & \mathbf{0} & \mathbf{0} & B_2 \end{bmatrix}$$

with the vectors

$$\begin{aligned} \underline{a}_1 &= \begin{bmatrix} -2 & 0 & 0 \end{bmatrix}^\top, \\ \underline{a}_2 &= \begin{bmatrix} -\frac{2}{3} & 0 & 0 \end{bmatrix}^\top \end{aligned}$$

and the matrices

$$\begin{aligned} B_1 &= \begin{bmatrix} \frac{12}{5} & -\frac{2}{5} & 0 \\ -\frac{2}{5} & \frac{2}{5}+\frac{2}{9} & -\frac{2}{9} \\ 0 & -\frac{2}{9} & \frac{2}{9}+\frac{2}{13} \end{bmatrix}, \\ B_2 &= \begin{bmatrix} \frac{2}{3}+\frac{2}{7} & -\frac{2}{7} & 0 \\ -\frac{2}{7} & \frac{2}{7}+\frac{2}{11} & -\frac{2}{11} \\ 0 & -\frac{2}{11} & \frac{2}{11}+\frac{2}{15} \end{bmatrix}. \end{aligned}$$

B Algorithmic Aspects

In this section, some implementational details for the fast evaluation of the preconditioning operation $C_3^{-1}\underline{w}$ (4.1) are presented. The preconditioning action requires the multiplication with the matrices W_p and $W_p^\top$ and a diagonal scaling with a Kronecker product between the diagonal matrices $\mathfrak{D}_M$ and $\mathfrak{D}_K$. Some steps can be performed before starting the solution process. The multiplication $W_p\underline{w}$ requires actually two muliplications,

- the basis transformation from the basis $[\tilde{L}_{(-2,2)}]$ into the basis $[\tilde{\Psi}_p] = [\tilde{L}_{(-2,2)}]\tilde{W}_p$, i.e. the multiplication with the matrix $\tilde{W}_p$, (3.35) and
- the multiplication with the eigenvector matrix G in (3.44).

The first one is performed by the routine

$\underline{y} = \texttt{trafo}(\underline{x}, p)$:	
Input:	polynomial degree p (odd) vector $\underline{x} \in \mathbb{R}^{2p-1}$, components ordered according to (A.1).
Output:	$\underline{y} \in \mathbb{R}^{2p-1}$.

- Set $n = p+1$, $k = \frac{p-1}{2}$ and $m = 2p-1$.
- Call $[\underline{r}, \underline{s}] = \texttt{auxiliary}(p)$.
- Set $\underline{h}_1 = [x_2, \ldots, x_{k+1}, x_1/2, x_{k+2}, \ldots, x_p]$ and $\underline{h}_2 = [x_{p+1}, \ldots, x_{p+k}, x_1/2, x_{p+k+1}, \ldots, x_m]$.
- Set $\underline{a} = \sqrt{2}(\underline{h}_1, \underline{r})\underline{s}$ and $\underline{b} = \sqrt{2}(\underline{h}_2, \underline{r})\underline{s}$.
- Call $\underline{u} = \texttt{trafo22}(\underline{h}_1, n)$ and $\underline{v} = \texttt{trafo}_\texttt{t}\texttt{22}(\underline{h}_2, n)$.
- Set

$$\begin{aligned} \underline{y} \;=\; & [u_{k+1} + v_{k+1}, a_1 + u_1, \ldots, a_k + u_k, a_{k+2} + u_{k+2}, \ldots, a_p + u_p, \\ & b_1 + v_1, \ldots, b_k + v_k, b_{k+2} + v_{k+2}, \ldots, b_p + v_p]\,. \end{aligned}$$

This subroutine calls $[\underline{x}, \underline{y}] = \texttt{auxiliary}(p)$, $\underline{x} = \texttt{trafo22}(\underline{y}, n)$ and $\underline{x} = \texttt{trafo}_\texttt{t}\texttt{22}(\underline{y}, n)$. The subroutine `auxiliary` computes two auxiliary vectors $\underline{x}, \underline{y} \in \mathbb{R}^p$, where p is odd:

- Set $m = \frac{p+1}{2}$, $\underline{h} = [0, \ldots, 0] \in \mathbb{R}^p$, $h(m) = 1$.
- Call $\underline{x} = \texttt{trafo22}(\underline{h}, p+1)$ and $\underline{y} = \texttt{trafo}_\texttt{t}\texttt{22}(\underline{h}, p+1)$.

The next routine is $\underline{x} = \texttt{trafo22}(\underline{y}, n)$. The input is the vector $\underline{y} \in \mathbb{R}^{n-1}$ which contains the coeffcients of a piecewise linear function f in the basis of the usual hat functions. Output are the coefficients of f in the used wavelet basis. The basis functions of the nodal and wavelet basis are ordered with respect to the midpoint of their support. The subroutine $\underline{x} = \texttt{trafo}_\texttt{t}\texttt{22}(\underline{y}, n)$ performs the transposed operation.
The matrix G has to be computed before starting the solution process. This requires two sparse matrices $\tilde{\mathfrak{D}}_M$ and $\tilde{\mathfrak{D}}_K$ in (3.39). They are computed via the subroutine $[\tilde{\mathfrak{D}}_M, \mathfrak{M}] = \texttt{genmass}(p)$ which computes the required entries in (3.39) of the matrix

$$\int_{-1}^{1} [\tilde{\Psi}_p]^\top [\tilde{\Psi}_p]\, \mathrm{d}x = \int_{-1}^{1} \tilde{W}_p^\top [\tilde{L}_{(-2,2)}]^\top \tilde{W}_p [\tilde{L}_{(-2,2)}]\, \mathrm{d}x$$

using the formula $\tilde{W}_p^\top M^{\tilde{L}_{(-2,2)}} \tilde{W}_p$.

$[\tilde{\mathfrak{D}}_M, \mathfrak{M}] = \texttt{genmass}(p)$	
Input:	polynomial degree p (odd)
Output:	diagonal part of $\tilde{\mathfrak{D}}_M$ dense block $\mathfrak{M}$ in (3.42)

- Call $M = \texttt{masslegendre}(p)$
- Call $[\underline{r}, \underline{s}] = \texttt{extension}(p)$
- FOR $I = 1, 2p-1$
  - $\underline{e} = [0, \ldots, 0] \in \mathbb{R}^{2p-1}$, $\underline{e}(I) = 1$.
  - Call $\underline{x} = \texttt{trafo}(\underline{e}, p)$
  - $\tilde{\mathfrak{D}}_M(I, I) = \underline{x}^\top M \underline{x}$
  - IF $\underline{r}(I) \neq 0$ THEN
    - FOR $J = 1, 2p-1$

· $\underline{g} = [0, \ldots, 0] \in \mathbb{R}^{2p-1}$, $\underline{g}(J) = 1$.

· Call $\underline{y} = \texttt{trafo}(\underline{g}, p)$

· IF $\underline{r}(J) \neq 0$ THEN $\mathfrak{M}(I, J) = \underline{y}^\top M \underline{x}$

∗ ENDFOR

– ENDIF

• ENDFOR

This subroutine calls $\texttt{masslegendre}(p)$ which computes $M^{\tilde{L}_{(-2,2)}}$ using the explicit structure given in (3.3). Note that the diagonal matrices $\mathfrak{D}_{M,-}$ and $\mathfrak{D}_{M,+}$ are saved in one diagonal matrix. The subroutine $[\tilde{\mathfrak{D}}_K, \mathfrak{K}] = \texttt{genstiff}(p)$ replaces `masslegendre` by a routine for the computation of $K^{\tilde{L}_{(-2,2)}}$. Once the structure of $\mathfrak{M}$ and $\mathfrak{K}$ is known, the matrix G is obtained as the eigenvector of the generalized eigenvalue problem $\mathfrak{K}\underline{x} = \lambda\mathfrak{M}\underline{x}$ (3.43), see also (3.44) and can be computed by the implicit QL-algorithm. This gives us also the matrices $\mathfrak{D}_M$ and $\mathfrak{D}_K$ in (3.47). For an efficient implementation, the matrices $\mathfrak{D}_M$ and $\mathfrak{D}_K$ can also be computed before once starting the solution process. Since $\mathfrak{M}, \mathfrak{K} \in \mathbb{R}^{m,m}$ with $m \approx \log_2 p$, the total cost for the generation of all matrices is $\mathcal{O}(p^2) + \mathcal{O}(p^2 \log_2^2 p) + \mathcal{O}(\log_2^3 p)$.

Acknowledgement: The author thanks Joachim Schöberl (RWTH Aachen) for initiating this work and Clemens Pechstein (JKU Linz) for reading the manuscript. This work has been supported by the Spezialforschungsbereich F013 "Numerical and Symbolic Scientific Computing" of the FWF, project F1306.

References

[1] M. Ainsworth. A preconditioner based on domain decomposition for *h-p* finite element approximation on quasi-uniform meshes. *SIAM J. Numer. Anal.*, 33(4):1358–1376, 1996.

[2] I. Babuška, A. Craig, J. Mandel, and J. Pitkäranta. Efficent preconditioning for the *p*-version finite element method in two dimensions. *SIAM J.Numer.Anal.*, 28(3):624–661, 1991.

[3] S. Beuchler. Multi-grid solver for the inner problem in domain decomposition methods for *p*-FEM. *SIAM J. Numer. Anal.*, 40(3):928–944, 2002.

[4] S. Beuchler. A domain decomposition preconditioner for *p*-FEM discretizations of two-dimensional elliptic problems. *Computing*, 74(4):299–317, 2005.

[5] S. Beuchler and D. Braess. Improvements for some condition number estimates in p-fem. *Num. Lin. Alg. Appl.*, 13(7):573–588, 2006.

[6] S. Beuchler, R. Schneider, and C. Schwab. Multiresolution weighted norm equivalences and applications. *Numer. Math.*, 98(1):67–97, 2004.

[7] J. Bramble, J. Pasciak, and J. Xu. Parallel multilevel preconditioners. *Math. Comp.*, 55(191):1–22, 1991.

[8] M. Costabel, M. Dauge, and L. Demkowicz. Polynomial extension for H^1, $H(curl)$ and $H(div)$ on a cube. Technical report, IRMAR, Rennes, 2007.

[9] W. Dahmen. Wavelet and multiscale methods for operator equations. *Acta Numerica*, 6:55–228, 1997.

[10] I. Daubechies. *Ten lectures on wavelets*, volume 61 of *CBMS-NSF Regional Conference Series in Applied Mathematics*. Society for Industrial and Applied Mathematics (SIAM), Philadelphia, PA, 1992.

[11] T. A. Davis, J. R. Gilbert, S. I. Larimore, and E. G. Ng. A column approximate minimum degree ordering algorithm. *ACM Trans. Math. Software*, 30(3):353–376, 2004.

[12] L. Demkowicz. *Computing with hp Finite Elements.* CRC Press, Taylor and Francis, 2006.

[13] M. O. Deville and E. H. Mund. Finite element preconditioning for pseudospectral solutions of elliptic problems. *SIAM J. Sci. Stat. Comp.*, 18(2):311–342, 1990.

[14] B. Guo and W. Gao. Domain decomposition method for the *hp*-version finite element method. *Comp. Methods Appl. Mach. Eng.*, 157:524–440, 1998.

[15] W. Hackbusch. *Multigrid Methods and Applications.* Springer-Verlag. Heidelberg, 1985.

[16] S. Jensen and V. G. Korneev. On domain decomposition preconditioning in the hierarchical $p-$version of the finite element method. *Comput. Methods. Appl. Mech. Eng.*, 150(1–4):215–238, 1997.

[17] G.M. Karniadakis and S.J.Sherwin. *Spectral/HP Element Methods for CFD.* Oxford University Press. Oxford, 1999.

[18] V. Korneev, U. Langer, and L. Xanthis. On fast domain decomposition methods solving procedures for *hp*-discretizations of 3d elliptic problems. *Computational Methods in Applied Mathematics*, 3(4):536–559, 2003.

[19] V. G. Korneev. Почти оптимальныи метод решения задач Дирихле на подобластях декомпоситсии иерархическои *hp*-версии. Дифференциальные Уравнения, 37(7):1008–1018, 2001. An almost optimal method for Dirichlet problems on decomposition subdomains of the hierarchical *hp*-version.

[20] J. Mandel. Iterative solvers by substructuring for the *p*-version finite element method. *Comput. Methods Appl. Mech. Eng.*, 80(1-3):117–128, 1990.

[21] J. M. Melenk, C. Pechstein, J. Schöberl, and S. Zaglmayr. Additive Schwarz preconditioning for *p*-version triangular and tetrahedral finite elements. *IMA J. Num. Anal.*, 2008. to appear.

[22] R. Munoz-Sola. Polynomial liftings on a tetrahedron and applications to the *h-p* version of the finite element method in three dimensions. *SIAM J. Numer. Anal.*, 34(1):282–314, 1996.

[23] L. F. Pavarino. Additive schwarz methods for the *p*-version finite element method. *Numer. Math.*, 66(4):493–515, 1994.

[24] L. F. Pavarino and O. B. Widlund. Iterative substructuring methods for spectral elements in three dimensions. In *Krizek, M. (ed.) et al., Finite element methods. 50 years of the Courant element. Conference held at the Univ. of Jyväskylä, Finland, 1993. Inc. Lect. Notes Pure Appl. Math. 164, 345-355* . New York, NY: Marcel Dekker , 1994.

[25] L.F. Pavarino and O. Widlund. A polylogarithimc bound for an iterative substructuring method for spectral elements in three dimensions. *SIAM J. Numer. Anal.*, 33(4):1303–1335, 1996.

[26] R. Schneider. *Multiskalen- und Wavelet Matrixkompression.* Teubner, 1998.

[27] C. Schwab. *$p-$ and $hp-$finite element methods. Theory and applications in solid and fluid mechanics.* Clarendon Press. Oxford, 1998.

[28] P. Solin, K. Segeth, and I. Dolezel. *Higher-Order Finite Element Methods.* Chapman and Hall, CRC Press, 2003.

[29] A. Toselli and O. Widlund. *Domain Decomposition Methods- Algorithms and Theory.* Springer, 2005.

[30] A. J. Wathen. An analysis of some element-by-element techniques. *Comput. Methods Appl. Mech. Eng.*, 74(3):271–287, 1989.